A Thesis

entitled

Development of a HILIC-MS Approach to Quantitative Measurement of Nicotinic Acid Adenine Dinucleotide Phosphate (NAADP)

by

AL Mughram, Mohammed Hassan M

Submitted to the Graduate Faculty as partial fulfillment of the requirements for the

Master of Science Degree in Medicinal Chemistry

_____

Dr. James T Slama, Committee Chair

_____

Dr. Erin G. Prestwich, Committee Member

_____

Dr. Katherine A. Wall, Committee Member

_____

Dr. Amanda Bryant-Friedrich, Dean
College of Graduate Studies

The University of Toledo

August 2018

An Abstract of

Development of a HILIC-MS approach to quantitative measurement of nicotinic acid adenine dinucleotide phosphate (NAADP)

Mohammed AL Mughram

Submitted to the Graduate Faculty as partial fulfillment of the requirements for the Master Degree in Medicinal Chemistry

The University of Toledo

August 2018

Nicotinic acid adenine dinucleotide phosphate, NAADP, is the most potent second messenger that triggers Ca^{+2} release from intracellular stores. To further understand the roles of NAADP, it will be useful to develop direct methods to measure endogenous levels of NAADP in resting cells and in addition to measure changes resulting from modulation of NAADP concentrations by stimuli. In general, the hydrophilic characteristic of nucleotides and the presence of (poly)phosphate moieties makes it difficult to separate these nucleotides under normal reversed phase conditions without using an ion-pairing agent, creating conditions that are incompatible with liquid chromatography-mass spectrometric analysis. We have successfully developed a liquid

chromatography-mass spectrometry method without the use of ion pairing agents. We have utilized an amine functionalized stationary phase and hydrophilic interaction chromatography (HILIC) to separate and quantitate NAADP in the presence of structurally related nucleotides, including NADP, NAD, AMP, ADP, and ATP. This HILIC method is joined to a single quadrupole mass spectrometer equipped with an electrospray ion source using negative ion mode. Using this system, we can detect as little as 2 pmol of NAADP in aqueous solution and are anticipating being able to use the method to determine NAADP concentrations in mammalian cells.

Table of Contents

List of Tables

List of Figures

List of Abbreviations

Ca^{+2} .....calcium ion

DL .....desolvation line

DAG.....diacylglycerol

ESI.....electrospray ionization

HB .....heat block
HILIC.....hydrophilic interaction liquid chromatography

IP-RP.....ion-pair reversed-phase

LOD .....limit of detection
LOQ .....limit of quantification

MRM.....Multiple reaction monitoring
m/z.....mass to charge ratio

NMR .....nuclear magnetic resonance

Pmol .....picomole

SIM .....selected ion monitoring

UV/VIS .....ultraviolet-visible spectroscopy

Chapter 1

Introduction

Ca^{+2} ions have numerous effects on and modulate functional aspects of all living cells. They govern and regulate activities of all eukaryotic cells. These ions play vital roles in signal transduction by acting as a second messenger. Ca^{+2} signaling occurs via the entrance of extracellular Ca^{+2} into the cytoplasm of cells or by the release of intracellular Ca^{+2} stores as a response to molecular messenger triggers. When Ca^{+2} signaling happens, vast changes in cellular behavior will occur, which can lead to different cellular responses such as contraction, secretion, fertilization, synaptic transmission, and transcription. Thus, Ca^{+2} as a universal intracellular regulator plays vital roles in intracellular and extracellular processes.

1.1 Intracellular Ca^{+2} triggers:

Inositol triphosphate (IP_3), cyclic ADP-ribose (cADPR), and nicotinic acid adenine dinucleotide phosphate (NAADP) are molecules that have been recognized as intracellular Ca^{+2} triggers. The IP_3 molecule is the first known Ca^{+2} -mobilizing second messenger and has been extensively studied since its discovery. Early in 1975, Dr. Robert

Michell hypothesized that there was a connection between the hydrolysis of phosphatidyl inositol-bisphosphate, PIP_2, and Ca^{+2} signaling.[1] He proposed that PIP_2 hydrolysis produced a product that was later identified as IP_3, which could induce the release of intracellular Ca^{+2} stores. Dr. Micheal J. Beridge tested out this hypothesis and found that PIP_2 was hydrolyzed into DAG and IP_3 via the action of the phosphodiesterase enzyme, phospholipase C. In 1981, he and his team demonstrated IP_3 acts as a second messenger after entering cytoplasm and mobilizing Ca^{+2} from the endoplasmic reticulum (ER).[2] In 2009, a review was published in which the timeline of IP_3 discovery as the first identified second messenger for mobilizing intracellular Ca^{+2} was shown.[3]

1.2 NAADP and cADPR as intracellular Ca^{+2} mobilizers:

Later in 1987, Dr. H.C.Lee discovered the pyridine derivative nucleotides, NAADP, and cADPR, as novel second messengers for mobilizing cellular Ca^{+2}**.** This discovery was made during studies of Ca^{+2} mobilizing pathways induced by different pyridine nucleotides in sea urchin eggs homogenate.[4] Indeed, cADPR and NAADP are pyridine derivative dinucleotides; cADPR is a metabolite of NAD, whereas NAADP is derived from NADP. The chemical structure of cADPR was determined early in 1989.[5] In 1991, Dr. Lee published an article to explain the enzymatic synthesis of cADPR from NAD via the catalytic activity of ADP-ribosyl cyclase.[6]

In 1995, the most potent Ca^{+2} mobilizing agent, NAADP, was isolated as a contaminant present in commercial NADP, and the Ca^{+2} releasing activity that was detected in sea urchin homogenates was originally attributed to this impurity in the sample.[7] In 1997, Dr. Lee published a review that discussed all the research that had been done on the both NAADP and cADPR dinucleotides during the first 10 years of the discovery of their Ca^{+2} signaling activities.[8]

1.3 Intracellular Ca^{+2} stores triggered by NAADP:

In the biochemical context, signaling occurs when cells are stimulated to trigger Ca^{+2} release from intracellular stores. Receptors on cell surfaces activate intracellular signaling pathways that mobilize Ca^{+2} from intracellular organelles through specific Ca^{+2}-releasing channels within cells.[9] Some subsequent studies after the discovery showed that the NAADP Ca^{+2}-releasing mechanism is different from the cADPR and IP_3-releasing mechanisms; in particular, NAADP stimulates Ca^{+2} stores that are distinct from those stimulated by cADPR and IP_3.[7]

IP_3 and cADPR mobilize Ca^{+2} from stores localized within the sarcoplasmic reticulum or the endoplasmic reticulum (ER) via inositol triphosphate and ryanodine receptor (RYR) activation, respectively.[10] On the other hand, the presence of independent

NAADP-sensitive Ca^{+2} stores have been controversial, and there is mounting evidences showing that NAADP releases Ca^{+2} from organelles known as acidic compartments/lysosomal-related stores.[10–13]

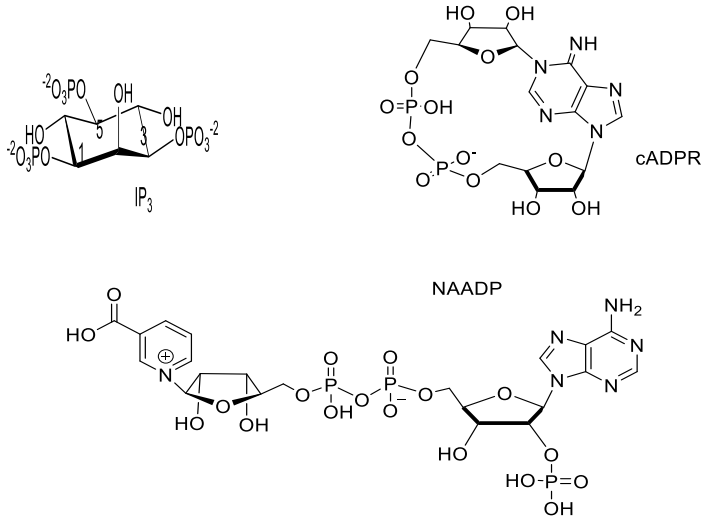

Figure 1: Chemical structures of IP_3, cADPR, and NAADP molecules that have roles in triggering Ca^{+2} release from intracellular stores.

1.4 Ca^{+2} release activity of NAADP:

Even with the small difference between the NAADP derivative and the known coenzyme NADP, which is only the substitution of nicotinic acid (NAADP) for nicotinamide (NADP), this modest change produces a dramatic difference in Ca^{+2} mobilizing activity of the NAADP molecule. When compared to the other previously

known IP_3 and cADPR Ca^{+2} mobilizers, NAADP has been identified as the most potent intracellular Ca^{+2} mobilizing agent that has been discovered.

Comparing NAADP Ca^{+2} mobilizing activity to other known intracellular calcium mobilizers, it was found that 50 nM NAADP caused a spike in intracellular Ca^{+2} amounts equal to the same amount elicited by 10 μM each of IP_3 or cADPR. [14]

1.5 NAADP Ca^{+2} release in sea urchin eggs:

The intracellular targets of NAADP were investigated primarily in sea urchin eggs. In sea urchin eggs, NAADP Ca^{+2}-sensitive stores were found to be separate from cADPR and IP_3 -sensitive stores. After treating sea urchin eggs with thapsigargin, (a sarcoplasmic/ER Ca^{+2}-ATPase inhibitor), NAADP was still able to trigger intracellular Ca^{+2} while IP_3 and cADPR showed no Ca^{+2}-releasing activities.[15] In another study, the caged compounds NAADP, IP_3, and cADPR were microinjected into sea urchin eggs that were already treated with thapsigargin; caged NAADP was efficiently photolyzed and triggered intracellular Ca^{+2}, while both caged IP_3 and cADPR showed no Ca^{+2}-releasing capabilities.[16]

In 2002, Churchill et al. investigated NAADP-sensitive Ca^{+2}-releasing stores in lysosomal-related organelles in sea urchin eggs. Intact sea urchin eggs were incubated with glycyl-L-phenylamine-2-naphthylamide (GPN), a cathepsin C substrate that disrupts

lysosomes, which have been proposed as NAADP's targeted organelles. A significant decrease in Ca^{+2} -mobilization was noticed and resulting from photolysis of caged NAADP; also, there was no Ca^{+2}-release resulting from free NAADP microinjection, While GPN did not interfere with Ca^{+2} release from caged IP_3 and cADPR photolysis.[17] In this study, selective disruption of lysosomes-related granules negatively affected the response of NAADP-Ca^{+2} targets in sea urchin eggs.

Indeed, early investigations of NAADP cellular targets in sea urchin eggs concluded that NAADP targets a distinct Ca^{+2} store, which appears to be located within lysosomal-related organelles, which are not related to the earlier investigated ER-associated IP_3 and cADPR-mediated calcium pathways.

1.6 NAADP Ca^{+2} release in mammalian cells:

1.6.1 NAADP releasing in acinar cells:

Studies of NAADP Ca^{+2}- induced release have been expanded to include mammalian cells with an attempt to determine whether NAADP targets the analog of reserve granules termed lysosome-like acidic granules also found in mammalian cells and also if it's working in a novel signaling pathway that is separate from IP_3 and cADPR-associated pathways. Exocrine acinar cells were one of the first cells types that had been used to

explore calcium-mediated signaling. The usual amount of Ca^{+2} in pancreatic acinar cells' ER is high in the resting state, and triggering of Ca^{+2} release would yield a high cytosolic Ca^{+2} spike with a decline in ER Ca^{+2} content.[18] In 1999, the first study was published in which it was reported that NAADP induced Ca^{+2} signaling in acinar cells.[14] NAADP was introduced into the cytosol of acinar cells by using a patch pipette in whole cell mode. In this study, Cancela et al. showed that 1-100 μM of NAADP was enough to cause NAADP receptor desensitization without Ca^{+2} release.[14] In the presence of μM concentrations of NAADP in the pipette solution, they found that caged NAADP photolysis failed to release intracellular Ca^{+2}; therefore, they concluded that μM concentrations of NAADP were sufficient to desensitize NAADP receptors. This suggests that the mammalian NAADP receptor has two binding sites, a high affinity stimulatory site, and a low sensitivity inhibitory site.

Inhibitors of cADPR and IP_3 failed to affect NAADP Ca^{+2} releasing responses in sea urchin eggs.[7] In acinar cells, it was found that these inhibitors abolished Ca^{+2} NAADP-induced spikes, which might be related to Ca^{+2} spikes associated with NAADP-activated ryanodine and IP_3 receptors. However, in the presence of inhibitory concentrations of NAADP (100 μM), the capability of IP_3 and cADPR to induce Ca^{+2} release was also tested. Cells were treated with 10 μM of IP_3 and cADPR each, and they were able to respond in the presence of an inactivating concentration of NAADP; these results showed that NAADP desensitization was not related to calcium-ion release through the IP_3 or ryanodine receptors.[14]

These two pieces of evidence taken together, it was hypothesized that NAADP induced Ca^{+2} release from specific NAADP-sensitive stores that lead to release of large ER Ca^{+2} through a mechanism related to ryanodine and InsP3 receptors, which is called the "trigger hypothesis''.

However, intracellular NAADP targets are still an area of interest for investigators, and mounting evidence has shown that the candidate receptor for NAADP is a lysosomal channel that is termed the two-pore channel (TPC).[13,19] TPCs are cation-selective ion channels that form a family of receptors in animal acidic organelles and plant vacuoles as well, in addition to being the only well-known Ca^{+2} channel that is present in animal and plant cells.[20]

1.6.2 NAADP release in cardiac cells:

In addition to the investigation of acinar cells, it has been shown in cardiac cells that NAADP was capable of binding with high affinity (130 μM and 4 nM) to two different sites of cardiac NAADP receptors.[21] It was clear that Ca^{+2} signaling in cardiac tissues is more complicated and that more receptors are involved in addition to the already known ryanodine receptors.[21] Based on this evidence and the complexity of Ca^{+2} signaling in this crucial organ, NAADP might participate in different cardiac functions. In 2012, it was shown that NAADP levels in cardiac tissues increased after beta-adrenergic agonist

stimulation [22], suggesting that beta-adrenergic agonist signaling might be related to NAADP-sensitive cardiac regulation.

1.6.3 NAADP release in T lymphocytes:

In T cell lines, NAADP releasing activities have been thoroughly investigated. Microinjection of NAADP into Jurkat T cell lines showed that low concentrations of NAADP (nM) evoked Ca^{+2} signaling, while, (μM) concentrations evoked no detectable spikes (inactivation response).[23] Most importantly, it was shown that using an inactivating concentration of NAADP led to blocking of the T cell receptor-CD3 complex -mediated Ca^{+2} responses, which indicates that NAADP-induced Ca^{+2} release is intrinsic to the mechanism of Ca^{+2} signaling in T cells. Ramadn Ali et al. reported a dominant role of NAADP in the activation, proliferation, and cytokine production in both naive and effector CD4 and CD8 T cells, which was not observed in the natural regulatory T cells.[24]

Recently, NAADP was shown to have a role in Ca^{+2}-dependent exocytosis activity of cytotoxic T lymphocytes (CTL).[25] In this study, NAADP was shown to activate the two-pore channels (TPCs) in target cells' immunological synapses and work as a specific messenger of exocytosis in the CTL lytic granules exocytosis.[23]

The complexity of intracellular Ca^{+2} stores and their channels make it difficult to obtain a comprehensive understanding of NAADP- Ca^{+2} signaling roles in different cells unless there was an integral picture of NAADP-induced Ca^{+2} release.

1.2 Assays for endogenous NAADP measurement:

Determination of cellular NAADP concentration is essential for identifying different cellular stimuli related to NAADP Ca^{+2} signaling and investigating its functions in different physiological roles. Up to date, enzymatic cycling [26,27] and competitive binding assays [28,29] have been established to measure cellular NAADP levels in various cells.

1.2.1 Enzymatic cycling assay:

The enzymatic cycling assay was originally developed in 2002 by Graeff and Lee in order to determine the amount of cADP-ribose in rat tissue extract.[30] The normal function of ADP-ribosyl cyclase is to catalyze cADPR synthesis from NAD; however, this novel cycling assay showed that it's possible to reverse the enzymatic synthesis and obtain NAD from cADPR in the presence of an excess amount of nicotinamide along with the action of ADP-ribosyl cyclase. This cycling assay detected femtomole levels of cellular cADPR, demonstrating high sensitivity.

In 2006, this enzymatic cycling assay was extended to measure cellular NAADP levels in human T lymphocytes.[27] Using of ADP-ribosyl cyclase, extracted cellular NAADP was converted in a reverse reaction to NADP in the presence of excess nicotinamide. NADP was then included in cycling reaction that was controlled by two

enzymes (1) glucose-6-phosphate dehydrogenase and (2) diaphorase. Glucose-6-phosphate (G6P)-dehydrogenase caused reduction of NADP into NADPH, and then NADPH was re-oxidized into NADP by diaphorase, which instantaneously converts resazurin to resorufin (fluorescent dye), the indicator reaction. Before the enzymatic cycling assay, any interfering endogenous NADP in the extract was removed using gravity-fed anion exchange chromatography and was then treated with a degradative enzyme (*Neurospora crassa* NADase) to remove any negligible amount of NADP that could be present. The NADase digestive enzyme can hydrolyze NADP into 2'-phospho-ADP-ribose but has no hydrolytic effects on NAADP.[30]

The basic exchange reaction in the enzymatic cycling assay using *Aplysia* cyclase should be done under acidic pH conditions, while the other coupled-enzyme assays were controlled in neutral pH. This indicated that the cycling assay had to be done using several steps involving pH neutralization and sample manipulation. In 2013, the enzymatic cycling assay was improved to become more effective with the mutation of Glu98 residue on the *Aplysia* cyclase to the uncharged glycine residue, E98G.[26] The E98G mutant form of the *Aplysia* cyclase enzyme was able to reversely catalyze the conversion of NAADP into NADP at neutral pH, which made this cycling reaction more straightforward than in previous experiments considering all enzymatic steps could be done concurrently.

1.2.2 Radioreceptor binding assay:

This assay is a competitive radioligand binding assay that was developed by taking advantage of the irreversible binding of NAADP to its uncharacterized receptor in the sea urchin eggs homogenates. The radioreceptor binding assay requires radiolabeled NAADP (^{32}P-NAADP). In 2004, Churamani et al. were able to measure cellular NAADP in human red blood cells, rat hepatocytes, and *Escherichia coli*. Cell extracts (containing unlabeled NAADP) were incubated with sea urchin egg homogenates prior to addition of ^{32}P-NAADP. Incubation of cellular extracts with the sea urchin homogenates prior to addition of the radiolabeled NAADP led to irreversible binding of cellular NAADP to the receptors. The subsequent addition of the radiolabeled NAADP can lead to cellular NAADP determination based on the percentage of radioligand binding inhibition. In 2007, Lewis et al. refined and improved the radioreceptor assay with successful determination of NAADP concentration under resting conditions and in response to stimulating agonists.[29]

The enzymatic cycling assay and radioreceptor binding assay were designed to quantify cellular NAADP. The enzymatic cycling assay is capable of determining the amount of cellular NAADP via an indirect method involving the conversion of NAADP to NADP followed by estimating the amount of NADP. In the enzymatic cycling assay, there was no need for synthesis of a radiolabeled compound; however, purification of the

sample using anion-exchange chromatography and enzymatic treatments are required before any measurements are made. On the other hand, the radiolabeled assay is the other available validated assay that could be used but requires synthesis of high specific activity radiolabeled NAADP. In Table 1, comparison of endogenous concentrations of NAADP and NADP using the enzymatic cycling and competitive binding assays published by Graeff and Lee in 2013.[26]

Table 1: Estimated cellular concentration of NAADP and NADP using binding and cycling assays:[26]

cell types extract	NAADP	NADP	assay used
1- Red blood cells.	66 nM	32 µM	Binding Assay
2- Red blood cells.	23 nM	21 µM	Cycling Assay
3- Rat hepatocytes.	18 nM	82 µM	Binding Assay
4- Rat liver.	97 nM	80 µM	Cycling Assay

1.3 Liquid chromatography-Mass spectrometry for analysis of cellular nucleotides

Introduction:

In the pharmaceutical field, high-performance liquid chromatography (HPLC) is an extremely useful tool in research and development processes related to molecular analysis, separation, and quality control processes. Coupling HPLC with a detection technique such as mass spectrometry (MS) provides a powerful tool for accurate and rapid identification and quantification of small molecules and endogenous metabolites, which leads to better bioanalytical data during early drug discovery and developmental processes.

In the past, liquid chromatography coupled to a UV detector was the optimal choice for metabolite profiling and quantification; however, with accelerated advancements in the analytical research field, HPLC-UV is not capable of meeting current and future analytical demands. Limitations in the specificity and sensitivity of HPLC-UV detection makes it a restricted and insufficient tool for new bioanalytical assay goals. Undeniably, MS is a valuable detection technique with respect to quantitative and qualitative analysis of components in matrices. For instance, qualitative analysis could be obtained with the possibility of detecting molecular weights of a different compound; it also provides more

accurate quantitative analysis compared to ultraviolet (UV) detection. Nowadays, the field of liquid chromatography (LC)-MS has been progressing rapidly and coincides with established approaches for detection, identification, and quantification of different drugs and metabolites.

Currently, LC-MS has been the method of choice in bioanalytical chemistry research, and the method is obtained from the combination of the useful separation tool, liquid chromatography, with the detection power of mass spectrometry.

Practically, the way of detecting a molecule using MS can be performed by converting an analyte molecule to an ionized form in the ion-source. Then the mass analyzer sorts ionized analytes based on their mass to charge ratios that would be measured and displayed by a detector.[31] Different MS ionization sources such as matrix-assisted laser desorption/ionization (MALDI), electrospray ionization (ESI), and electron ionization (EI) can be used to ionize molecules of interest; therefore, different compounds' molecular masses, polarity, and thermal stability are crucial for choosing the suitable ionization mode. However, the usual ion-source used for biological molecules is ESI.[31]

1.3.1 Mass Spectrometry-based analysis of Nucleotides and dinucleotides:

Nucleotides and their metabolites are involved in various crucial cell functions, enzyme activation, and metabolism. Adenosine nucleotides such as adenosine triphosphate, diphosphate, and monophosphate (ATP, ADP, and AMP) are essential biomolecules that provide cells with energy and substrates that are incorporated in

numerous biochemical cellular processes. [32] In the same manner, nicotinamide nucleotides like NAD and NADP are known as redox cofactors that are present in cells in oxidized (NAD^+/$NADP^+$) and reduced (NADH/NADPH) forms. These coenzymes participate as electron carriers in reversible oxidation and reduction that are known as redox reactions.[33] The cellular redox state can be a valuable indicator of different normal and pathological cellular conditions, including in diseases such as diabetes and cancer.[34] Because of these conditions, intracellular nucleotide concentrations can be hugely affected as a result of cellular function abnormalities in addition to the use of treatments. Determination of cellular nucleotides and their metabolites is important for further understanding the rules involved in cellular functions in addition to the diagnosis of disorders related to deficiencies in cellular nucleotide levels.[35]

To date, development of approaches using HPLC and LC-MS instruments have become widely applicable for the concurrent determination of desired nucleotides in biological samples; separation techniques can be coupled to UV and MS detectors to be used in qualitative and quantitative profiling of endogenous nucleotides. Nowadays, development of approaches using UV detectors have become limited, which is mainly related to the low nucleotide sensitivity and specificity when using UV.[36] On the contrary, MS detection of cellular nucleotides has become an extremely important analytical tool in this field.

1.3.2 Chromatographic retention of nucleotides:

Cellular nucleotides such as ATP, ADP, and AMP and pyridine-derived dinucleotide: NAD, NADP, and NAADP are very hydrophilic nucleotides resulting in poor retention of these molecules using reversed phase (RP)-HPLC technique coinciding with early elution of peaks and poor resolution.[31] Likewise, anion-exchange chromatography is undesirable due to incompatibility with MS analysis because of the use of high salt concentrations such as trifluoroacetic acid/trifluoroacetate leading to MS ion suppression and contamination of the instrument.

In general, HPLC with UV detection provides more solvent choices that meet the requirements of different analytical approaches; on the contrary, when using MS as a detector, more restrictions and limitations should be considered in choosing MS-compatible mobile phases. The mobile phase must be volatile, and use of phosphate buffer must be avoided entirely. Typical volatile mobile phases that can be used and be compatible with LC-MS would be either methanol or acetonitrile with water followed by addition of mobile phase modifiers such as ammonium formate or ammonium acetate buffers, and additives such as acetic or formic acid, and ammonium hydroxide to adjust the solvent pH.

Several approaches have been developed to detect and quantify endogenous nucleotides using LC-MS. Because of poor nucleotide retention on reversed phase columns, ion-pair chromatography is a very successful technique for increasing nucleotides retention and separation on reverse phase columns.[37] Different alkylamines such as dibutylamine [38], tributylamine [39,40,37], and dimethylhexylamine [41] were used as ion pairing reagents and were successful in achieving good chromatographic separations of different nucleotides. However, use of ion-pairing agents is undesirable and leads to ion suppression that results from the presence of nonvolatile solutes in the LC eluent that can lead to changes in the properties of droplet formation at the ESI interface.[42] Ion-pairing agents are also very hard to wash and clear away from instruments. Even with trace amounts of an ion-pairing reagent, the following applications' sensitivity could be affected. Therefore, the ion pair (IP)-RP technique could be applied only in cases in which an LC-MS instrument is dedicated for ion-pair reagent LC-MS work. These disadvantages can be resolved by using hydrophilic interaction liquid chromatography (HILIC) technique. Indeed, HILIC is currently the choice for analyzing highly hydrophilic molecules using LC-MS instruments.[43]

1.3.2.1 Retention of nucleotides in the reversed-phase mode:

As previously mentioned, HPLC coupled to MS has become the first choice for profiling pyridine and adenine nucleotides in biological matrices. The high polarity of nucleotides and similarity in structures in the presence of (poly)phosphate moieties make it difficult to separate different nucleotides without the help of ion-pairing agents.[31]

Previous detection of NAADP using LC-MS was only reported in the literature with the use of 20 mM dimethylhexylamine (DMHA) as an IP-agent.[41] It was successfully separated and quantified along with 20 other nucleotides in the RP mode. The optimal conditions for stability, peak shape, and resolution, included DMHA in the mobile phase at pH 7. Nucleotide detection and quantification was accomplished using LC-MS/MS with ESI in the negative mode.

In another metabolomics analysis using an IP reagent, Shimadzu published a review that showed a simultaneous analysis of 57 metabolites using an LCMS-8040 quadrupole mass spectrometer.[37] The analysis was done on a MASTRO C18 column with 10 mM of tributylamine and successfully detected and quantified different pyridine derivative dinucleotides (NAD, NADP, NADPH, and NADH) with a total run of 13 minutes. Indeed, all previous studies using RP-HPLC-MS for profiling pyridine dinucleotides and different cellular nucleotides used IP reagents such as dibutylammonium acetate [44], tetrabutylammonium acetate [40,39], and dibutylamine [38] to improve retention times and peak resolution.

1.3.2.2 Retention of nucleotides in the HILIC mode:

HILIC is an alternative LC technique used to improve polar metabolite retention times and avoiding the use of ion pairing agents. The term HILIC originated in 1990 to differentiate it from normal-phase separation.[45] In contrast to the reversed phase system,

the HILIC gradient starts with a high percentage of organic solvent (the weakly eluting solvent), and a low percentage of the aqueous buffer (the strongly eluting solvent). The most successful use of HILIC for metabolite analysis was achieved by Bajad et al. [43]. In this study, 142 water-soluble metabolites were detected and quantified by using seven different columns for both RP- and HILIC modes. Cyano, silica, and amino HILIC columns were tested at three different pH conditions (pH 2.8, 5.8, and 9, respectively). The aminopropyl column in the HILIC mode showed the best detection for approximately 118 nucleotides compared to the other stationary phases. Recently, a new approach was developed by using a Phenomenex LUNA NH2 column for a quantitative determination of NAD^+ metabolome in glial cell extracts.[46] Seventeen nucleotides were successfully quantified using ESI-MS/MS detection.

Other studies compared the efficiency for LC-MS analysis of polar nucleotides using HILIC and IP-RP-HPLC techniques. Michopoulos et al. showed that IP-RP-HPLC, with tributyl ammonium as an ion-pairing agent, and provided an optimized method to analyze polar ionic nucleotides using LC-MS in different urine, serum, and tissue samples.[39] In this study, a Waters Xbridge amide column was chosen to perform the HILIC studies. Peak tailing was observed with (poly)phosphorylated metabolites, and an increase in peak tailing coincided with an increase in nucleotide phosphorylation degree. Despite that, resolution was achieved for key metabolites such as the reduced and oxidized forms of NAD and NADP, and mono-, di-, tri-adenosine phosphates nucleotides.[39]

In a different study, un untargeted metabolomic analysis utilized a SeQuant ZIC-HILIC column to identify metabolites in a *Trypanosoma brucei* extract. Researchers successfully profiled about 20 nucleotides and nucleosides in addition to diverse types of metabolites such as amino and organic acids, and amines.[47]

A ZIC-HILIC column coupled with tandem mass spectrometry was also successfully used to analyze nucleotides from plant leaf extracts.[47] With the continuous development of LC-MS approaches for metabolic profiling using the HILIC chromatographic system, it appears that it will become a superior choice for improving retention and separation of polar metabolites, especially in cases in which IP-RP separation techniques would be contraindicated.

1.3.3 NAADP-mass spectrometry literature review:

Available studies providing analytical information for NAADP using mass spectrometry are limited. The first description of NAADP as the most potent Ca^{+2} releasing messenger included the characterization of NAADP using fast atom bombardment mass spectrometry (Fig. 2).[7] In 2007, NAADP was reported in a paper describing alternative MS/MS strategies for metabolite identification (Fig. 3) [48] using a Fourier transform ion cyclotron resonance mass spectrometry (FTICR-MS). The last study was performed using an IP-LC-MS/MS method, and NAADP was observed in a standard sample of nucleotides without biological detection (Fig. 4).[41]

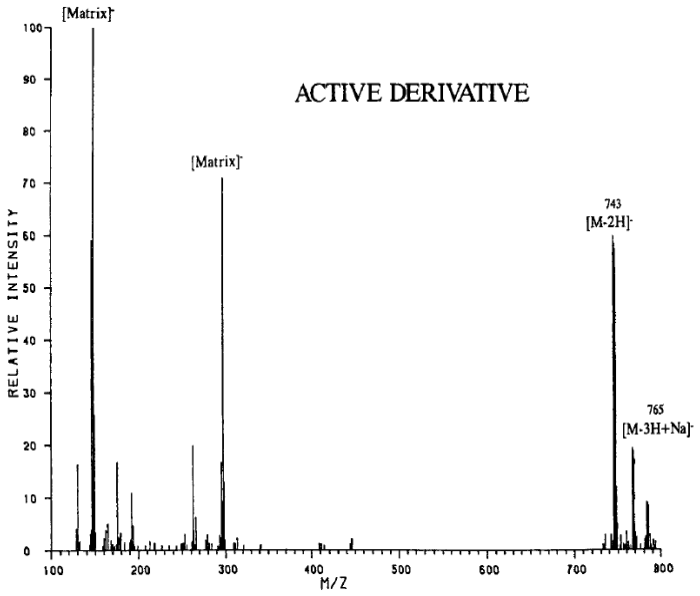

Figure 2: Mass spectra of NAADP obtained by using fast atom bombardment mass spectrometry.[7]

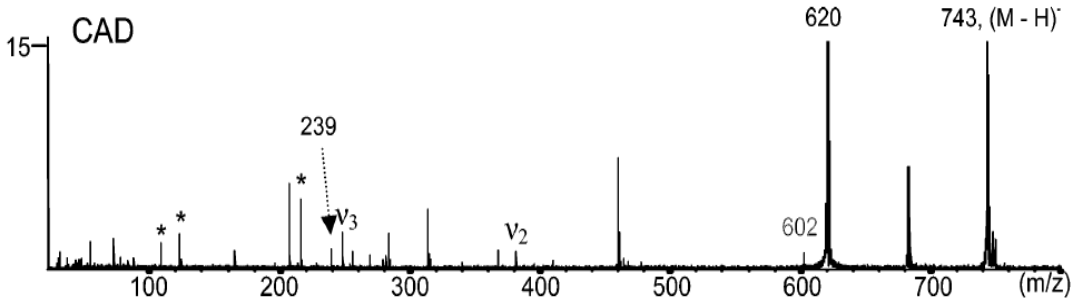

Figure 3: MS/MS spectra of NAADP using a Fourier transform ion cyclotron resonance mass spectrometry (FTICR-MS). [48]

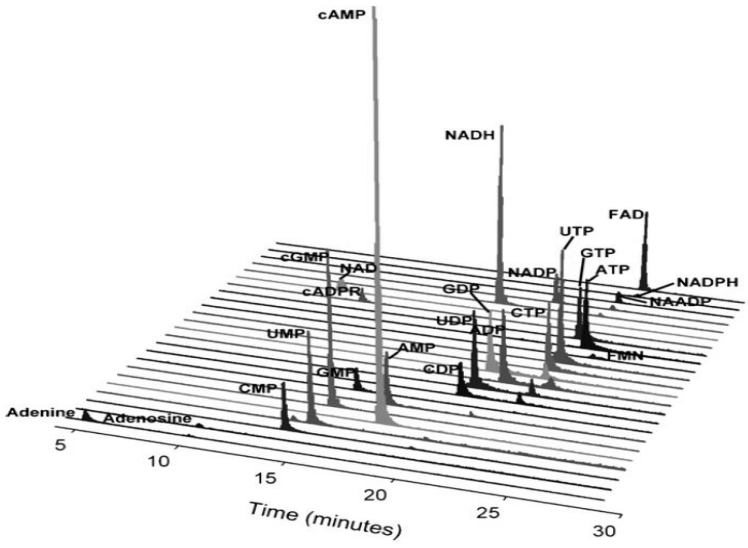

Figure 4: LC-MS/MS analysis using MRM scan showing the simultaneous detection of NAADP and related phosphate-containing metabolites in standard solution. [41]

1.3.4 Thesis overview:

Cells have numerous Ca^{+2} stores that can be triggered by the different Ca^{+2} messenger molecules. NAADP is the newest as well as the most potent Ca^{+2} mobilizing second messenger discovered to date. Understanding of its intracellular functions as a Ca^{+2} releasing second messenger has been challenging, because of the shortage and complexity of available NAADP-measurement assays. The need for a direct, sensitive, and straightforward assay for endogenous NAADP measurement is necessary for a better biological understanding of its Ca^{+2}-releasing functions. The development of an LC-MS approach can provide a more convenient, straightforward assay for this purpose and overcome the time-consuming and demanding processes that are required for the currently available NAADP-measurement assays.

The initial objective of this work was to: (1) identify preferred chromatographic separation conditions using an HPLC instrument that efficiently retain and separate NAADP from other related nucleotides in standard samples using MS-friendly environment; (2) Utilize a single quadrupole liquid chromatograph spectrometer (LCMS-2020) for further NAADP-mass spectrometric developments and optimizations.

In order to reach these objectives, enzymatic synthesis of NAADP was performed

in vitro by using a base exchange reaction. Highly pure NAADP was thus assured for subsequent chromatographic and mass spectrometric development processes. It also included the primary goal of investigating several chromatographic stationary phases and identifying an optimum and reproducible LC method that enabled the study of the ionization of NAADP in comparison to the related analytes as well as developing an LC-MS approach that would provide a promising new tool for the quantitative studies of endogenous NAADP.

Chapter 2

Results and discussion

2.1 Synthesis of NAADP:

The enzymatic synthesis of NAADP was carried out *in vitro* through a base exchange reaction (Fig. 5). The enzyme ADP-ribosyl cyclase was used to catalyze the exchange of nicotinamide group of NADP with nicotinic acid producing NAADP.[49] The pH of reaction medium plays a significant role in this enzymatic reaction. By adjusting pH to 4 and conducting the enzymatic exchange in the presence of an excess amount of nicotinic acid, the base-exchange reaction will be the predominant reaction with converting NADP to NAADP (Fig. 6).

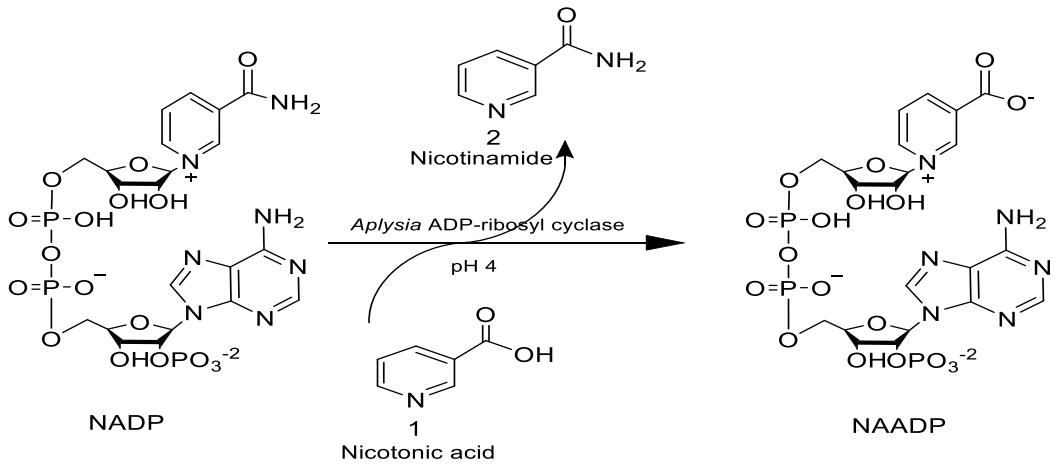

Figure 5*:* Scheme is showing the base exchange reaction catalyzed by *Aplysia* ADP-ribosyl cyclase. The nicotinamide group of NADP was exchanged by the nicotinic acid at pH 4.

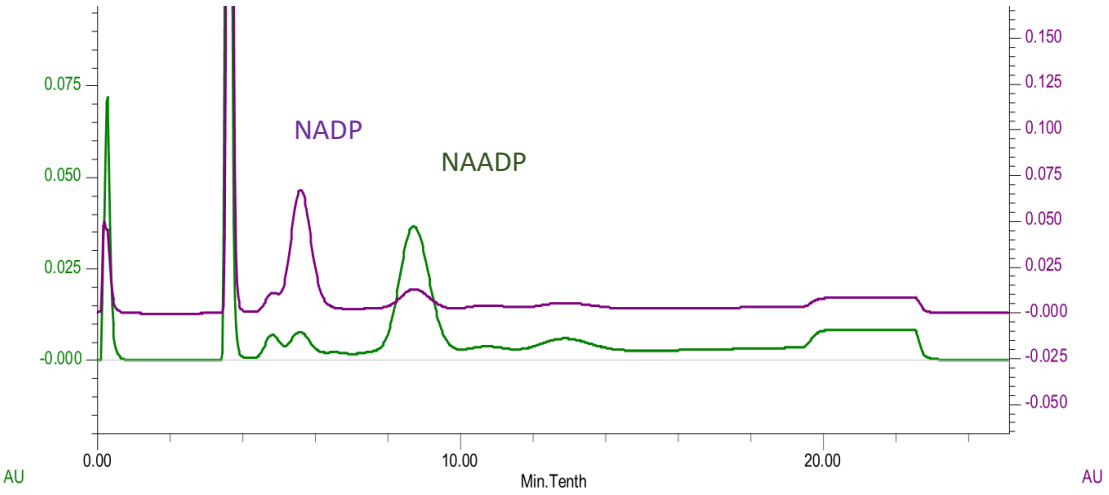

Figure 6: The enzymatic synthesis of NAADP from NADP using the base exchange reaction. The chromatograms show the progress of the enzymatic synthesis at the beginning of the incubation (Violet chromatogram), and after the converting of NADP to NAADP (green chromatogram). HPLC analysis of NAADP performed on AGMP-1 column described in Section (4.1.1). Solvents: A: H_2O, B: 100 mM TFA. Gradient: 0% B (2 min) – 45% B (17 min) – 100% B (17.10 min) – 100 % B (20 min) – 0% B (20.10 min). Flow rate: 3 mL/min.

2.2 Synthesis of deuterated NAADP (D_4-NAADP):

For dependable LC/MS analysis, internal standards are essential to overcome any instrument variations that occur from run to run as well as to control for isolation efficiency of the biomolecule of intersest. An internal standard should be structurally as similar as possible to an internal analyte. For this purpose, deuterated (D_4)-NAADP was enzymatically synthesized to be used as an internal standard (Fig. 7). Using of deuterated molecule as an internal standard is a convenient choice because of its simple synthesis and low cost, compared to ^{13}C and ^{15}N labeled standards. Heavy atom labeled standards

are usually more costly and require more elaborate syntheses. D_4-NAADP was a new compound that was first described in this work. The enzymatic synthesis was carried out using the base exchange reaction that was similarly used for the NAADP synthesis (Fig. 8).

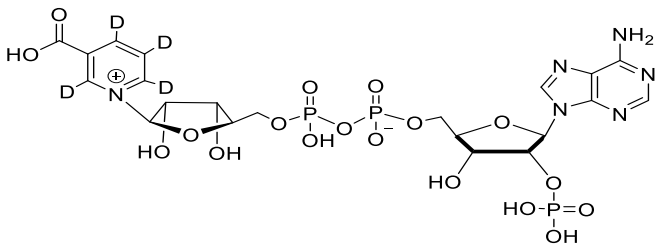

Figure 7: Chemical structure of the D_4-NAADP molecules.

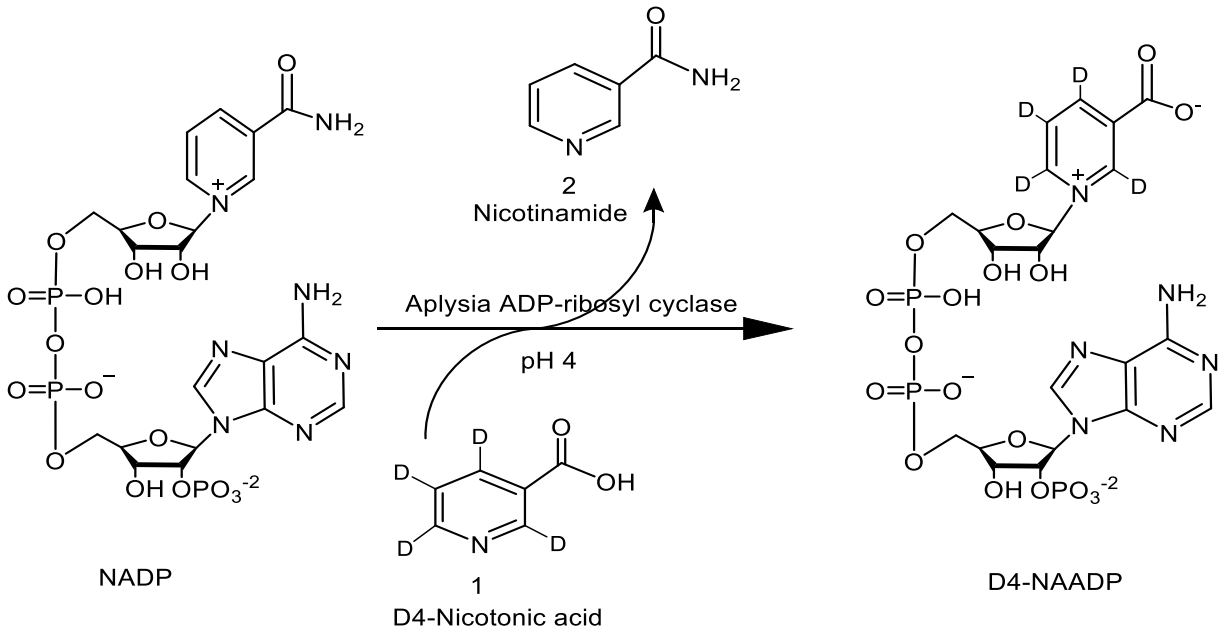

Figure 8: The enzymatic synthesis of D_4-NAADP using the base exchange reaction. The nicotinamide group of NADP was exchanged by deuterated nicotinic acid with catalyzing of the cyclase enzyme.

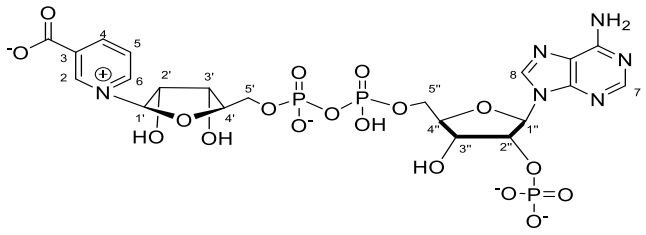

Table 2: ^{1}H NMR characterization for NAADP and d_4-NAADP *:

Proton location	NAADP	d4-NAADP
Nicotinate ring protons		
H_N2	9.16 (s, 1H)	
H_N4	8.78 (d, 1H, J=8.8)	
H_N5	8.10 (m, 1H)	
H_N6	9.08 (d, 1H, J=6.2)	
Adenine ring protons		
H_A7	8.45 (s, 1H)	8.48 (s, 1H)
H_A8	8.25 (s, 1H)	8.21 (s, 1H)
Anomeric protons		
H_N1'	6.20 (d, 1H, J= 5 Hz)	6.20 (d,1H, J= 5.7 Hz)
H_A1''	6.05 (d, 1H, J= 5.6 Hz)	6.05 (d, 1H, J= 5.16 Hz)
Pyridinium-ribose protons		
H2'	4.10-4.23 (m, 1H)	4.18-4.42 (m, 1H)
H3'	4.10-4.23 (m, 1 H)	4.18-4.42 (m, 1H)
H5'	4.10-4.23 (m, 2H)	4.18-4.42 (m, 2H)
H4'	4.50 (s, 1H)	4.50 (s, 1 H)
Adenine-ribose protons		
H2''	5.10 (m, 1H)	5.10 (m, 1H)
H3''	4.60 (m, 1H)	4.62 (m, 1H)
H4''	4.10-4.23 (m, 1H)	4.18-4.42 (m, 1H)
H5''	4.10-4.23 (m, 2H)	4.18-4.42 (m, 2H)

* The ^{1}H NMR Spectrum of NAADP in our experiment was recorded on a 600 MHz instrument using D_2O as the solvent.

2.4 HPLC development:

2.4.1 Chromatographic separation of NAADP and other nucleotides:

Ion-exchange chromatography is the popular chromatographic system that has been used for analyzing and separating NAADP as well as detecting and profiling different nucleotides in biological extracts. Because of the incompatibility of this chromatographic system with the liquid chromatography-mass spectrometric analysis, it was essential to develop a new chromatographic separation system that is compatible with the LC-MS analysis and provide a sufficient separation as well as enough mass spectrometry sensitivity for detection of cellular NAADP. Development of an LC method using low flow rates, volatile buffers and additives is critically required for LC/MS compatibility and sensitivity. For these reasons, various kinds of stationary phases had been tested in both the RP and HILIC modes to identify the optimum chromatographic retention and separation of NAADP from other structurally related nucleotides using equipment friendly MS-solvents. According to current studies, use of ion pairing-agents in the reversed phase mode is the primary technique that has been used to profile cellular nucleotides. However, because of the incompatibility of using non-volatile salts with available LC-MS instruments, the IP-RP technique was excluded in spite of its efficacy in improving hydrophilic compound retention in RP-HPLC mode. Mobile phases chosen to carry the HPLC and LC-MS work were solvent (A) H_2O with 0.1% formic acid and solvent (B) acetonitrile with 0.1% formic acid in the RP-HPLC mode. In the HILIC

mode, the aqueous phase was solvent (A) 10 mM ammonium acetate at pH 9.8, and the organic phase was solvent (B) acetonitrile. Chromatographic conditions including tested columns, mobile phases, gradient elution, and flow rates were tested using the SHIMADZU LC-20AT HPLC system and described in Section (4.5 and 4.6).

2.4.1 Reversed-Phase separation on C18 columns:

Octadecyl (C18) columns are usually the first-choice of columns for establishing new reversed-phase separation methods. C18 refers to the alkyl chain length that is bound to the silica surface in the column, where increasing the alkyl chain coincided with increasing the retention and selectivity of compounds with hydrophobic properties. Two silica-based columns with octadecyl ligands were tested in this experiment. The first column was a Waters Atlantis column (150 mm × 4.6 mm, particle size 5 µm), and the second column was a Phenomenex Synergi Fusion-RP column (100 mm × 3 mm, particle size 2,6 µm). Unlike traditional C18 columns, Synergi Fusion-RP and Waters Atlantis columns were designed and optimized to achieve a balance in retention of both polar and non-polar compounds.

2.4.2 Reversed-phase separation on phenyl stationary columns:

Silica particles bounded to phenyl groups would provide selectivity based on hydrophobic interactions between aromatic and unsaturated groups. Pi electrons of phenyl ligands would provide π–π interactions with aromatic rings of analytes, and that could improve nucleotide retention and separation. In our project, two phenyl-type stationary phases were tested in the reversed phase mode, a Phenomenex Kinetex biphenyl column (250 mm × 4.6 mm, 5 µm particle size) and a Phenomenex Synergi Polar-RP column (100 mm × 2 mm, 2.5 µm particle size).

2.4.3 Chromatographic separation on HILIC columns:

The hydrophilic interaction liquid chromatography (HILIC) system was developed as a procedure to separate compounds that are very hydrophilic and display poor retention on reversed phase columns. There are five classes of HILIC stationary phases, unfunctionalized silica, amino-bonded phase, amide-bonded phase, cationic and zwitterionic-bounded phases. In this study, a Phenomenex HILIC Kinetex column (100 mm × 4.6 mm, 2.6 µm particle size) and a Phenomenex Luna NH2 column (50 mm × 3 mm, 5 µm particle size) were tested using the HILIC chromatographic mode. All HPLC columns and conditions used are listed in Table 3.

Table 3: Chromatography columns and conditions tested:

Column Name (Suppliers)	Column Type	Dimensions (particle size)	Chromatography mode tested	pH tested
1-Atlantis dC18 column. (Waters)	Di-functionally bonded C18 ligands.	150 mm × 4.6 mm, 5 µm	RP	2.8[1]
2-Synergi Fusion-RP (Phenomenex).	A low ligand density polar embedded C18.	100 mm × 3 mm, 2.6 µm	RP	2.8
3-Biphenyl column (Phenomenex).	Biphenyl with TMS end-capping.	250 mm × 4.6 mm, 5 µm	RP	2.8
4-Synergi Polar- RP (Phenomenex).	Ether-linked phenyl (PH)	100 mm × 2 mm, 2.5 µm	RP	2.8
5-Kinetex HILIC column (Phenomenex).	Silica	100 mm × 4.6 mm, 2.6 µm	HILIC	2.8
6-LUNA NH2 (Phenomenex)	Aminopropyl	50 mm × 3 mm, 5 µm	RP, HILIC	5.8[2], 8.8[3], 9.8

[1] pH 2.8: 0.1% formic acid in both solvent A and solvent B.

[2] pH 5.8, pH 9.8: 10 mM ammonium acetate + acetic acid

[3] pH 8.8, pH 9.8: 10 mM ammonium acetate + ammonium hydroxide

2.5.1 Retention studies on the various RP-columns:

In the RP mode, standard nucleotides (ATP, ADP, NADP, NAD, and NAADP) exhibited poor retention on the Synergi Fusion-RP column. The mobile phase consisted of solvent (A) H_2O + 0.1% formic acid and solvent (B) acetonitrile + 0.1% formic acid. Under the conditions tested, the Synergi Fusion column was not able to provide sufficient retention of our standard nucleotides. Early co-elution of nucleotides was observed, and that would make it impossible to detect and quantify endogenous NAADP using the MS in the presence of other related metabolites such as NADP, NAD, ATP, AMP, and NAD.

The other C18 column that was investigated in the reversed mode was the Atlantis dC18 column. The mobile phase consisted of solvent (A) H_2O + 0.1% formic acid and solvent (B) acetonitrile + 0.1% formic acid. Packing materials of dC18 were designed to provide good retention properties of both polar and non-polar compounds. It is also compatible with 100% aqueous phase with superior stability compared to other traditional C18 columns. On this column, our nucleotides were retained; however, this stationary phase was unable to separate NAADP and NADP. Acetonitrile was replaced by MeOH in the mobile phase to explore any retention and resolution improvements; separation efficiency and retention time of nucleotides did not show any improvements when MeOH was substituted for acetonitrile.

Using the biphenyl column, limited success in the separation and retention of NAADP and other nucleotides was obtained. The mobile phase consisted of solvent (A) H_2O + 0.1% formic acid and solvent (B) acetonitrile + 0.1% formic acid. The packing material of the biphenyl column was designed to be 100% aqueous-compatible for use in retention of hydrophilic aromatic compounds. Because of the high polarity of nucleotides, they were barely retained on C18 reversed phase columns, and it was challenging to show sufficient retention and separation characteristics among other traditional C18 packings. In contrast, the biphenyl stationary phase enables a chromatographic separation of NAADP, ATP, ADP, NADP, and NAD to be achieved, even though asymmetric peak shapes were observed for NAADP and NADP (Fig. 9). The biphenyl stationary phase showed specificity and selectivity in the separation of the tested nucleotides compared to the C18 stationary phases. The slight retention of NAADP, NADP, ADP, ATP, AMP by the biphenyl stationary phase allowed elution of those nucleotides under isocratic conditions using 100 % aqueous solvent followed by a subsequent linear gradient to 20 % of the organic solvent for NAD elution. However, it must be mentioned that peak tailing of NAADP and NADP was observed using the biphenyl stationary phase under both isocratic and gradient conditions (Fig. 10). More importantly, we observed that the retention times of NAADP and NADP varied from run-to-run, even when we made an effort to maintain identical conditions. The peak tailing and the retention time variations made the use of this stationary phase unsuitable for our analysis of NAADP.

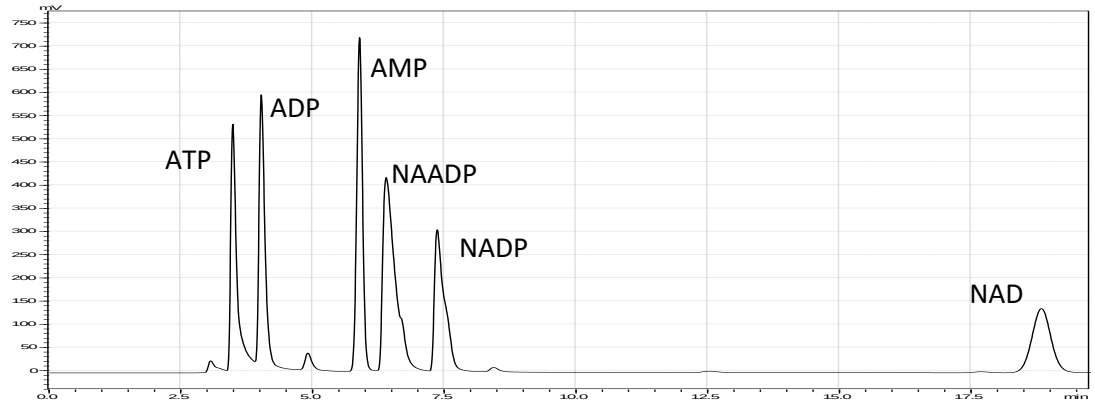

Figure 9: Reversed phase separation of standard mixtures of nucleotides using the biphenyl column (150 mm × 4.6 mm, 5 µm) at flow rate: 0.8 mL/min. Solvents: A: H_2O + 0.1% formic acid, B: acetonitrile + 0.1% formic acid. Gradient: 0 %B (0 min) – 0 %B (15 min) – 20 %B (20 min) – 95 %B (30 min) – 95 %B (40 min) – 0 %B (40.10 min) – 0 %B (60 min).

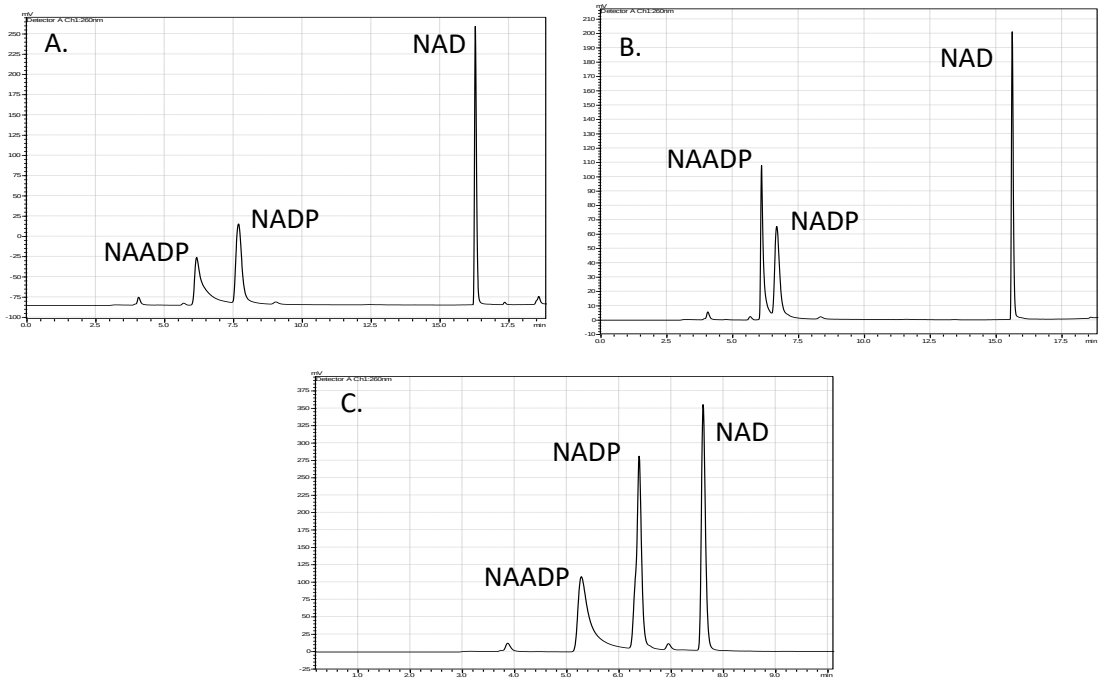

Figure 10: Reversed-phase separation of 0.5 mM standard sample of (**NAADP**, NADP, and NAD) on the Kinetex biphenyl column (250 mm × 4.6 mm, 5 µm particle size) using an isocratic elution (A, B) and gradient elution (C) chromatography. Flow rate: 0.8 mL/min.

Table 4: Gradient and isocratic elution chromatography tested for nucleotide separation on the biphenyl column:

Gradient A		**Gradient B**	
0.8 ml/min		0.8 ml/min	
Time (min)	%B	Time (min)	%B
0	0	0	0
10	8	10	0
15	20	15	20
25	95	25	95
35	95	35	95
35.10	0	35.10	0
55	0	55	0

2.5.2 Retention studies on HILIC columns:

Separation of nucleotides in the HILIC mode can be an excellent choice for developing an LC method to retain very hydrophilic compounds using an ESI-MS friendly solvent system. Two stationary phases were tested in the HILIC mode and under the conditions that were described in Section (4.5). Under the HILIC system, a silica-based stationary phase column (Kinetex HILIC column) showed severe peak tailing and lack of nucleotide separation. The severity of peak broadening coincided with the degree of phosphorylation of nucleotides (Fig.11). Moreover, NAADP was eluted within the same time frame as ATP-elution time and other nucleotides, which would make it

difficult to detect and quantify NAADP in a biological sample. Peak broadening of NAADP and different multiple phosphorylated nucleotides made this stationary phase inappropriate for carrying out LC-MS work.

A LUNA NH2 column was the second HILIC column which was evaluated and we show that it successfully achieved excellent chromatographic retention and separation for all tested nucleotides (Fig. 12). Acetonitrile (solvent B) was used as the non-eluting solvent of the mobile phase system. 5 mM and 10 mM ammonium acetate adjusted to pH 5.8, 8.8, and 9.8 was used as the high eluting power aqueous phase (solvent A). At pH 5.8 and 8.8, the interaction of nucleotides with the column stationary phase was found to be strong, and nucleotides could not be appropriately eluted. However, pH 9.8 was found to be the optimum condition, and nucleotides were sufficiently retained and eluted successfully. Adding 10 mM of ammonium acetate was found to be the lowest salt concentration that provided a reproducible chromatographic separation (Fig. 13). The chemical structure of -NH2 stationary phase is illustrated in Figure 11.

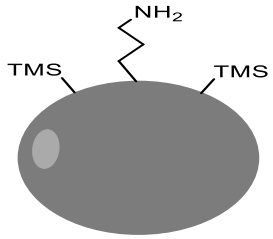

Figure 11: Chemical structure of -NH2 column

2.5.3 Chromatographic separation of NAADP with the utilization of an amine stationary phase:

A state-of-the-art in the separation of NAADP from NADP, NAD, ATP, ADP and AMP is presented in Figure 12. The special characteristic of the hydrophilic interaction of nucleotides with the stationary phase on this column enabled the successful retention and separation of NAADP from the other nucleotides. While the interaction of nucleotides with the amino-containing stationary phase was shown to be strong, using 80% organic solvent (acetonitrile) was shown to be the optimum condition for a proper elution. Table 5 describes the analytical conditions of the HILIC method.

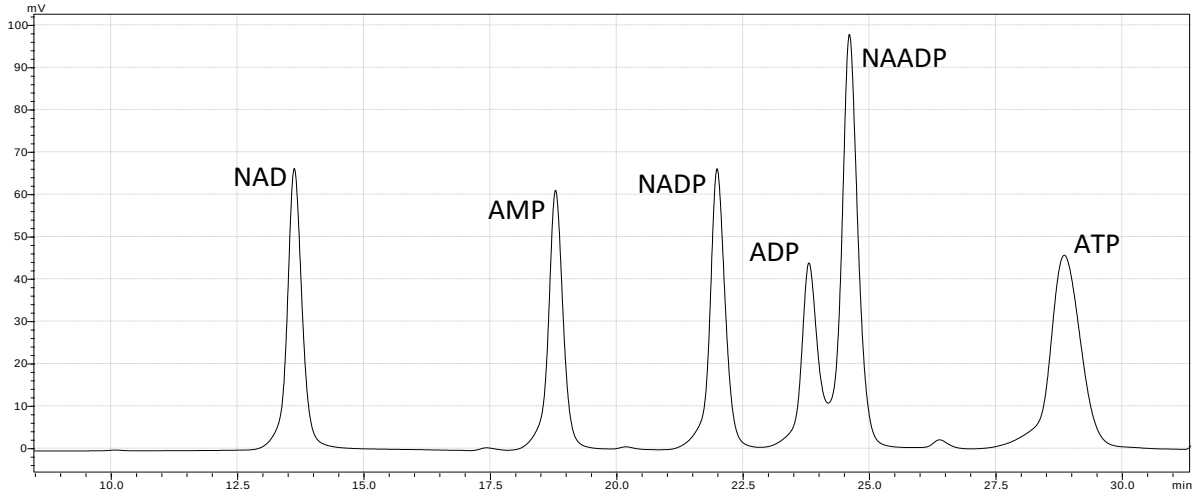

Figure 12: Optimized HPLC separation of a standard mix of NAD, AMP, NADP, ADP, NAADP, and ATP using the LUNA NH2 column at pH 9.8 in the HILIC mode.

Table 5: HPLC system (Shimadzu)

Column	Phenomenex Luna NH2 (5 µ, 50 mm × 3 mm)
Mobile phase	A: 10 mM ammonium acetate, ammonium hydroxide (pH 9.8) B: Acetonitrile.
Gradient condition	80 % B (0 min) – 0 % B (20 min) – 0 % B (30 min) – 80 % B (30.10 min) – 80 % B (48 min)
Flow rate	0.2 mL/min
Column temperature	Room temperature

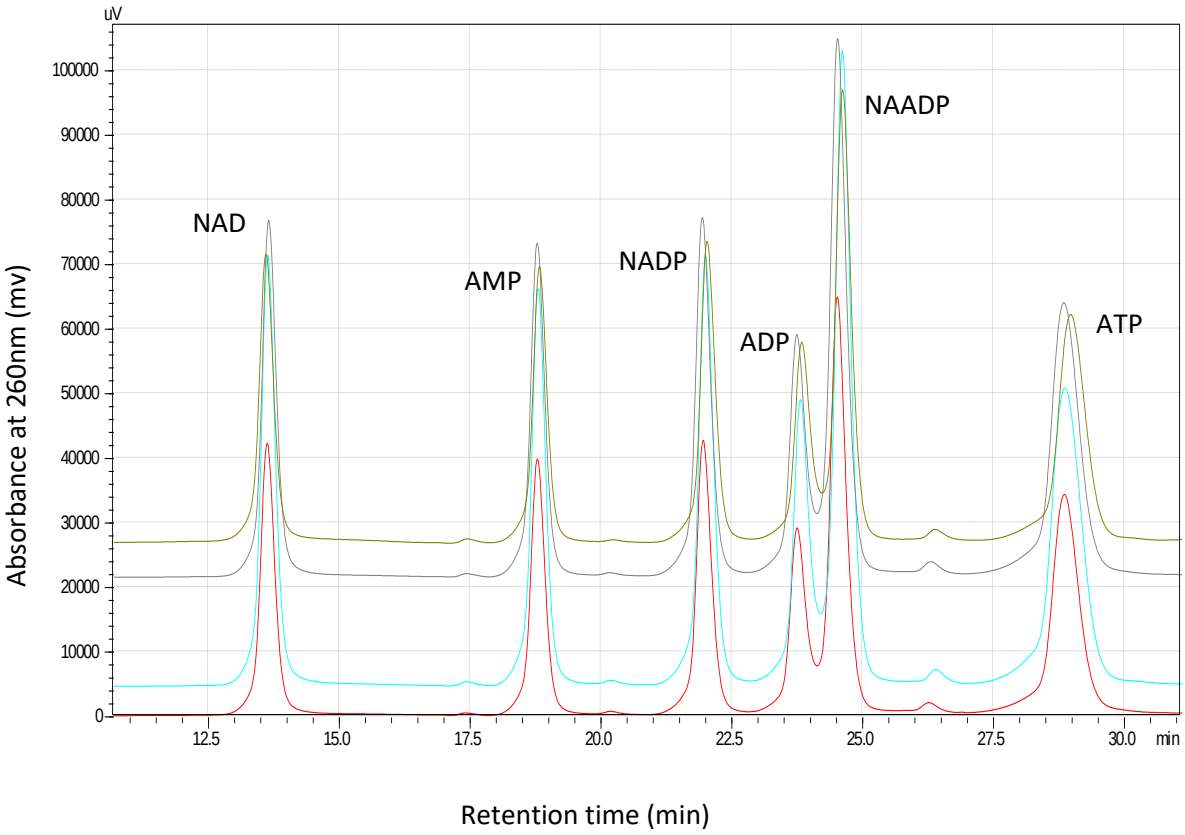

Figure 13: Reproducible chromatographic results of a 100 µM standard mixture of NAD, AMP, NADP, ADP, **NAADP** & ATP using LUNA NH2 column (50 mm × 3 mm) in the HILIC mode at pH 9.8. Solvents: A:10 mM of ammonium acetate, B: acetonitrile. flow rate: 0.2 mL/min. HPLC optimization conditions as described in Table 5.

2.6 Mass spectrometry development:

The LC-MS analysis of NAADP and other nucleotide standards were performed on an LCMS-2020 Single Quadrupole Chromatograph Mass Spectrometer (SHIMADZU). This mass spectrometer contains a single quadrupole mass filter and can work in a selective mode known as Selected Ion Monitoring (SIM). The ESI technique was employed for ionization processes in the negative and SIM modes throughout this study. Figure 14 shows a schematic view of the Electrospray Ionization source that was used. Optimized parameters of mass spectrometric detection of NAADP molecule are described in Table 6.

Table 6: optimized detection parameters for NAADP in ESI-MS analysis using negative ionization and SIM modes on a Shimadzu LC-MS 2020.

	NAADP
Molecular formula	$C_{21}H_{27}N_6O_{18}P_3$
Observed mass	743 m/z
Ionization probe	ESI
Polarity	Negative
Analysis mode	SIM
Drying gas flow	11 L/min
Nebulizer gas	1.5 L/min
DL temperature	200 °C
HB temperature	500 °C

2.6.1 Electrospray ionization (ESI):

The LC/MS utilizes an ionization and inlet system that allows eluents to move from the chromatographic system directly into the MS for detection. Some papers have reviewed and sufficiently explained the principle of the ESI process [50]. Briefly, the ionization process starts with infusion of the LC eluent through an inlet capillary that is located in the atmospheric pressure region of the ESI interface (Fig. 14). The principle behind the electrospray technique is the presence of a high voltage power supply that is connected from the metal capillary into the mass spectrometer across the atmospheric pressure region. A positive or negative voltage would be chosen according to the analytes. Applying high voltage to the capillary that carries the LC eluent would lead to the formation of a Taylor cone at the capillary surface that emits charged droplets; these droplets are detached from the capillary tip to form the initial droplets that move through the atmospheric pressure interface toward the mass spectrometer. Rapid solvent evaporation takes place in the ion evaporation region; this evaporation is assisted by a counterflow of heated nitrogen gas leading to fine droplets formation and clearing away of any uncharged materials. Ions are formed in solution before arriving at the ESI interface.

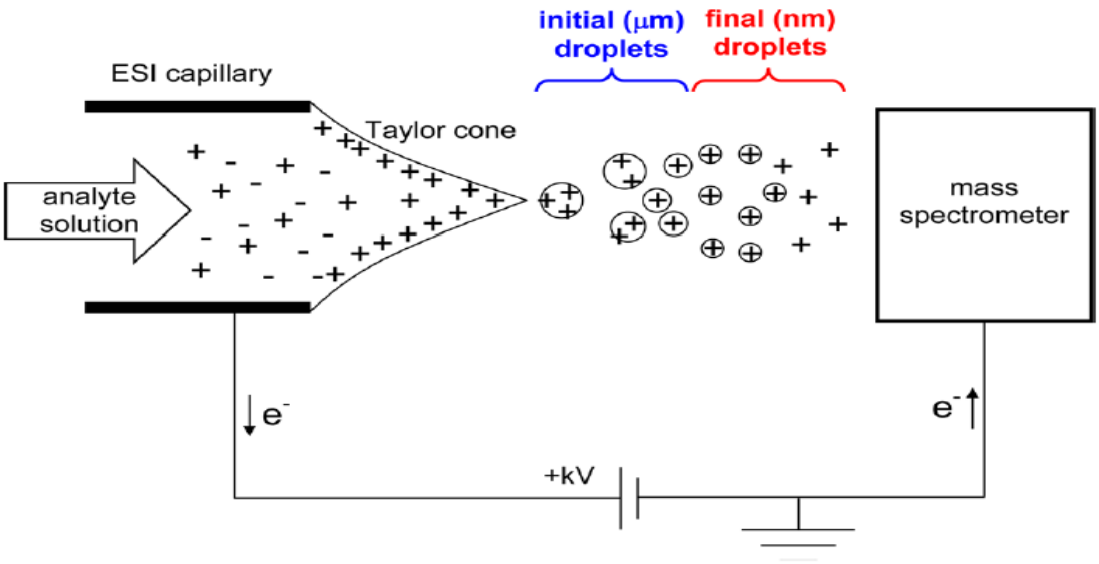

Figure 14: Schematic view of the electrospray ionization process. (Reprinted with permission [50], copyright 2013, American Chemical Society).

2.6.2 Solvent pH effects on ESI-MS efficiency:

The pH of mobile phase is one of several parameters that can affect the ESI-MS ionization efficiency for molecules. Therefore, we investigated the responsiveness of NAADP under different pH conditions using 10 mM ammonium acetate at pH 5.75, 8,75 and 9.8. NAADP was injected directly into the LC-MS; the quantitative analysis was performed under SIM and negative ion modes. Estimating the responsiveness of ionization was achieved by integrating the area under the curve of the NAADP (molecular ion; 743 m/z) signal under the tested pH conditions. It was observed that ESI-MS responsiveness efficiency was

directly proportional to the basicity of the solvent pH. The difference in NAADP-ionization efficiency showed a slight improvement among different aqueous solvent pH conditions that we had tested; however, pH 9.8 of solvent A was the optimum condition for NAADP ionization efficiency.

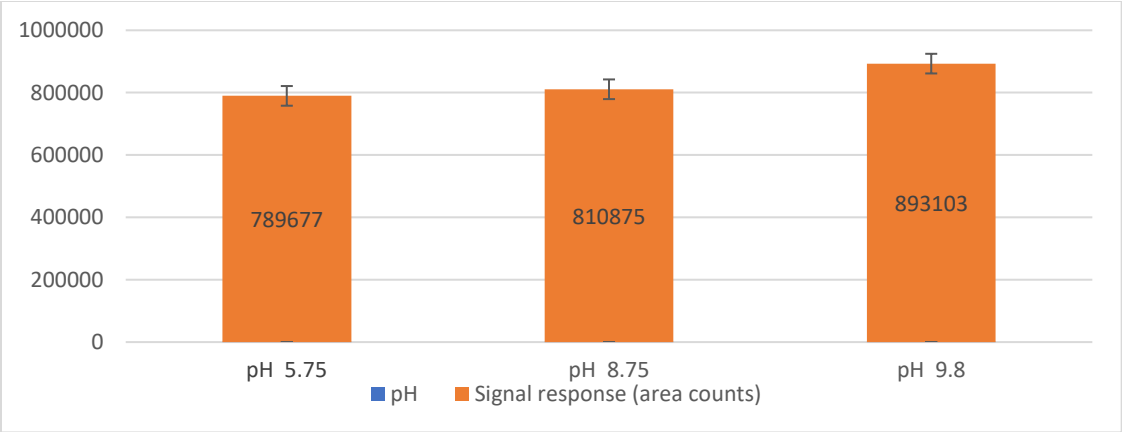

Figure 15: Investigation of the influence of the aqueous solvent pH on the ESI-MS ionization efficiency of NAADP. 10 mM of ammonium acetate aqueous solvent adjusted to pH 5.75, 8,75 and 9.8 conditions and analyzed using LC-MS 2020.

2.6.3 Mass spectrometric detection of NAADP:

NAADP ionization using the ESI process was evaluated in both positive and negative ion modes using full scan analysis. Determination of the optimum mode was achieved with a direct injection of 100 pmol NAADP into the ESI-MS. In general, the positive operating mode showed a lower intensity of $[M+H]^+$ ions coincided with producing more fragment ions. On the other hand, ESI negative

mode was the better operation mode, and that is because of the stronger strength of $[M-H]^-$ ions and lower limit of fragmentation in compared to the ESI^+ mode. Based on that, ESI^- mode was chosen to carry out the operation mode in the MS work (Fig. 16).

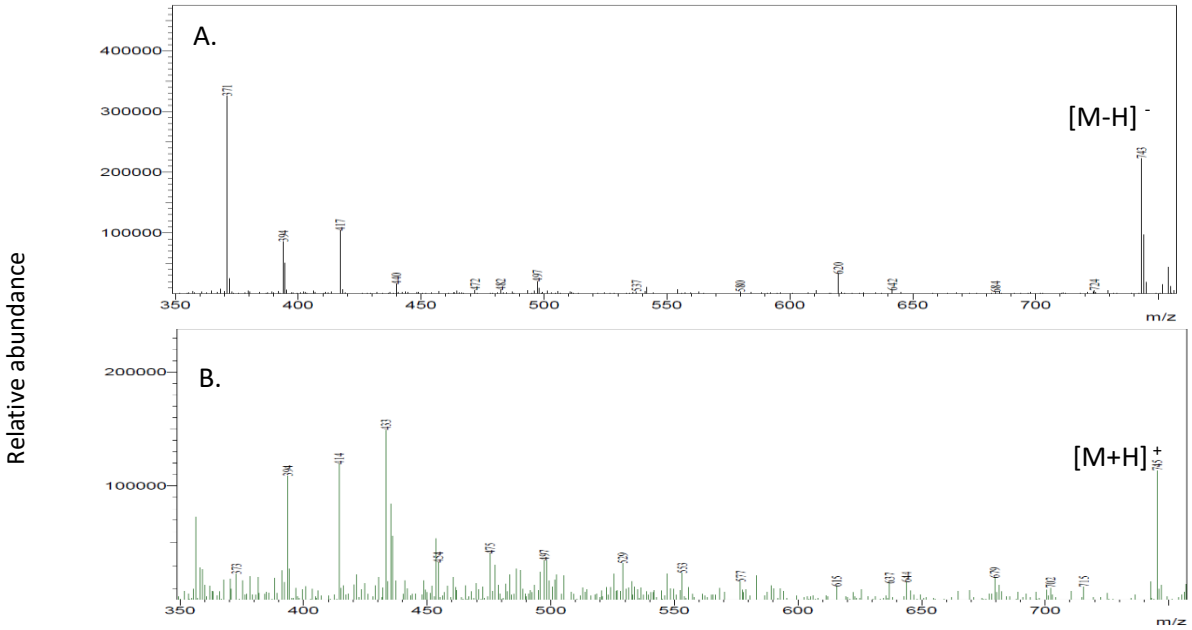

Figure 16: The observed mass spectra of NAADP (full scan analysis) with (A) negative and (B) positive electrospray ionization modes carried out on the LC/MS 2020 using direct injections of standard NAADP, 100 pmol. The intensities of $[M-H]^-$ ions were stronger than those observed for $[M+H]^+$ ions. Solvents: A: 10 mM of ammonium acetate (90 %), B: acetonitrile (10 %). flow rate: 0.2 mL/min.

2.6.4 Mass spectrometry detection:

In this work, LCMS 2020 was used for the LCMS development work, including NAADP detection, optimization, and quantification as well as identification of the monoisotopic masses of NADP, NAD, ATP, ADP and AMP nucleotides. ESI in negative and SIM detection modes were carried out on the LCMS-2020 for this work.

The monoisotopic masses of NAADP and other standards that were used, were calculated according to the molecular formulas that are shown in Table 6. Observed spectrum masses were 743 m/z for NAADP, 742 m/z for NADP, 506 m/z for ATP, 426 m/z for ADP and 346 m/z for AMP. All standard nucleotides were ionized as single charged ions in the negative mode which was confirmed by the molecular weight of nucleotides and the observed isotopic patterns. Quantification analysis was performed using LabSolutions software (2008-2016 Shimadzu Corporation) based on peak area of extracted ions. NAADP showed low ionization/detection efficiency using the ESI technique in compared to other analytes in the standard sample.

2.6.5 HILIC-MS method for quantifying NAADP:

The ability to separate NAADP, NADP, NAD, ATP, ADP, and AMP using the amino stationary phase and an MS friendly mobile phase enabled the simultaneous quantitative analysis of each of the nucleotides (Fig. 17). Nucleotide retention times were shown to be consistent from run to run after sufficient pre-run equilibration time (Fig. 13).

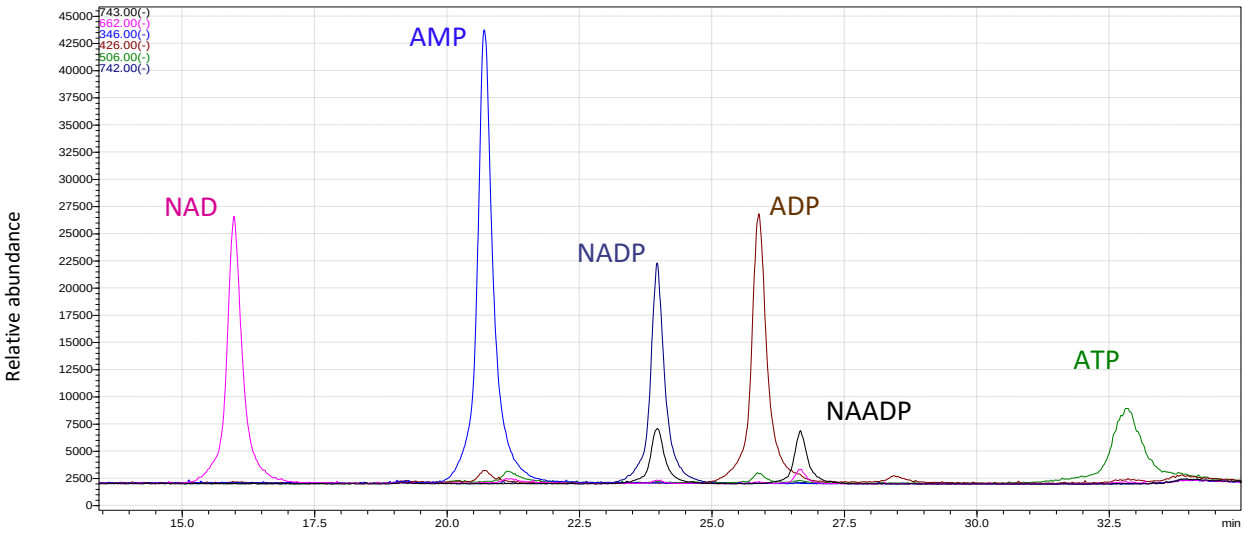

Figure 17: Mass chromatogram of LC-MS analysis using SIM and negative modes showing the simultaneous detection of NAD, AMP, NADP, ADP, NAADP, and ATP in 100 µM standard solution.

The LC method coupled to a single quadrupole mass spectrometer permitted the quantitative analysis of NAADP and the other structurally-related nucleotides. All standards used for the LC/MS development process were re-purified utilizing the biphenyl column, the purification step was necessary to remove any contamination that can be resulted from the nucleotide hydrolysis. Calibration curves are shown in Fig 18, Fig 19, Fig 20, Fig 21, and Fig 22. Linear regression was used to fit a linear equation to the measured points. The value of correlation coefficient, r^2, close to 1 indicates a proper fitting and confirms the linear correlation between the analyte concentration and signal peak. The r^2 value for NAADP was higher than 0.99 in our method. The parameters limit of detection (LOD) and limit of quantitation (LOQ) for analytes were determined

statistically based on the standard deviation of nucleotide responses at low concentrations and the slope of the calibration curve with applying three determinations at four or more concentrations. The results of detection and quantitation limits were obtained and recorded in table 7. An overview of the analytical characteristics of NAADP and other nucleotides using the HILIC-MS method is reported in Table 7.

Table 7: A HILIC-MS method for quantifying of NAADP and other nucleotides:

Analytes	Parent ion formula	Precursor ion $[M-H]^-$ (m/z)	Retention Time (min)	Correlation Coefficient (r^2)	Detection limit LOD (pmol)	LOQ
NAADP	$C_{21}H_{27}N_6O_{18}P_3^-$	743	26.8	0.992	2	6
NADP	$C_{21}H_{27}N_7O_{17}P_3^-$	742	24	0.99	0.5	1.5
NAD	$C_{21}H_{26}N_7O_{14}P_2^-$	662	15.9	0.994	0.4	1
ADP	$C_{10}H_{14}N_5O_{10}P_2^-$	426	25.7	0.998	0.3	1
AMP	$C_{10}H_{13}N_5O_7P^-$	346	20.7	0.996	0.3	0.8

LOD= 3.3 σ / Slope.

LOQ = 10 σ / Slope.

σ: The standard deviation of the response at low concentrations.
Slope: The slope of the calibration curve.

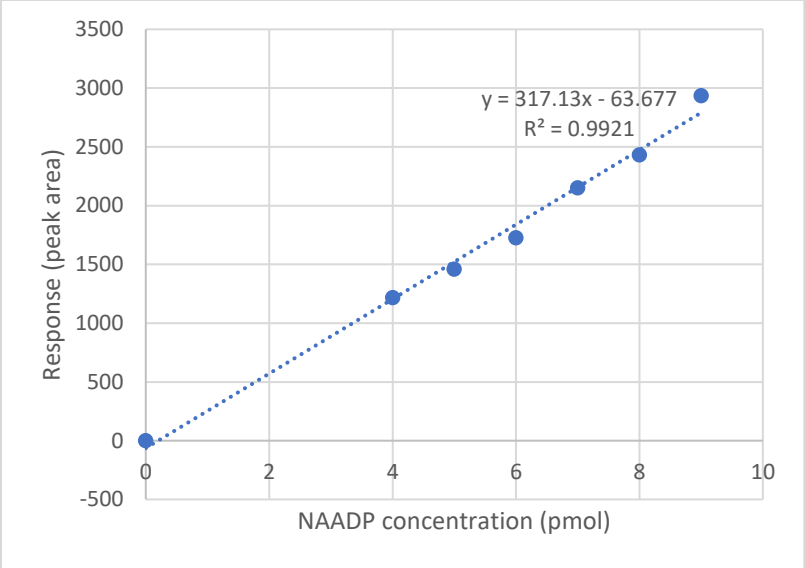

Figure 18: Calibration curve for the quantification of NAADP in the range of 4-9 pmol by LC-MS using the HILIC-ESI-MS method.

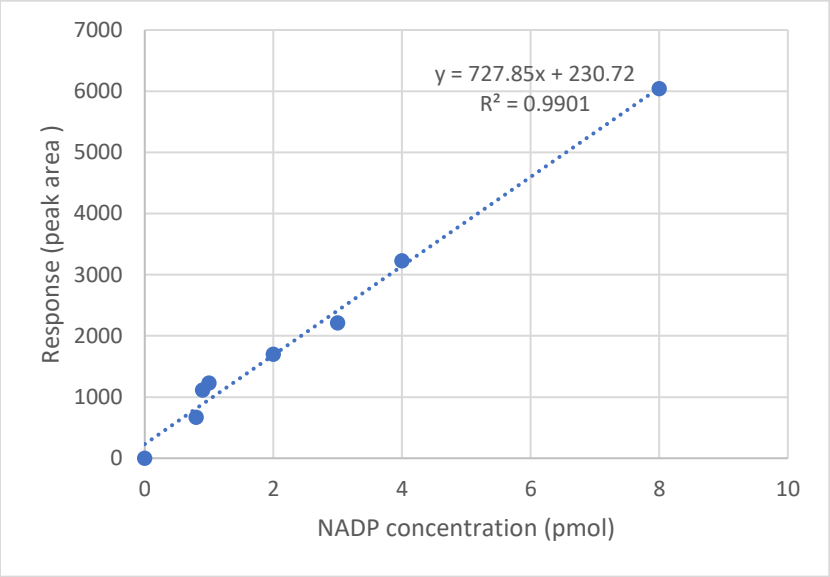

Figure 19: Calibration curve for the quantification of NADP in the range of 0.8 - 8 pmol by LC-MS using the HILIC-ESI-MS method.

.

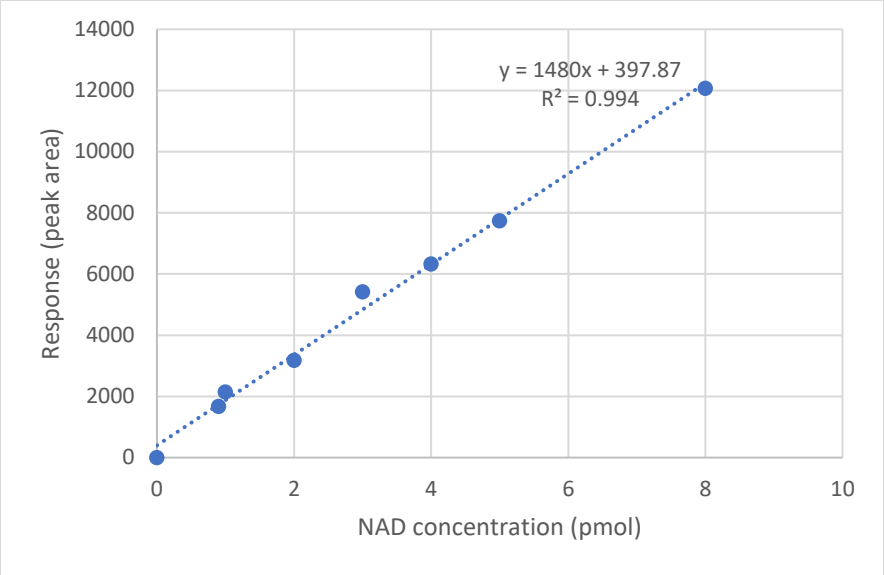

Figure 20: Calibration curve for the quantification of NAD in the range of 0.6 - 8 pmol by LC-MS using the HILIC-ESI-MS method.

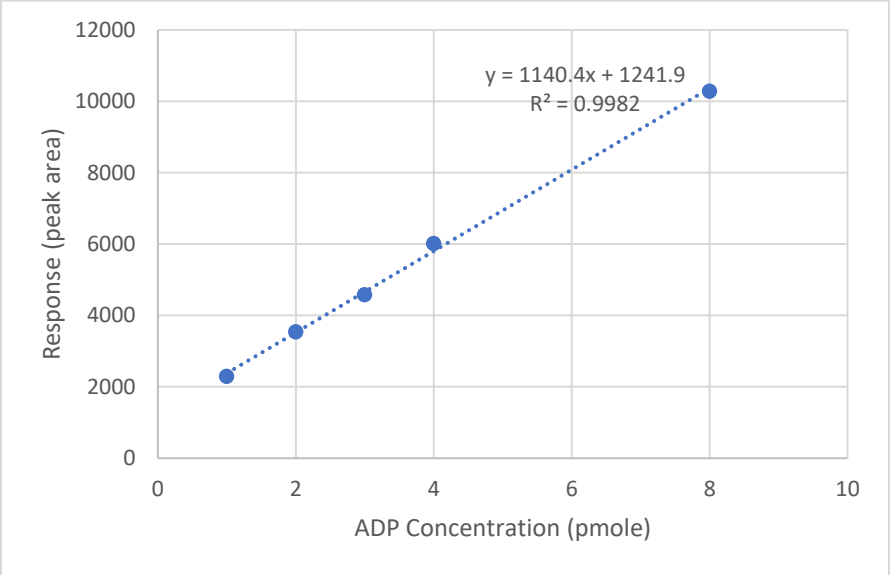

Figure 21: Calibration curve for the quantification of ADP in the range of 0.8 - 8 pmol by LC-MS using the HILIC-ESI-MS method.

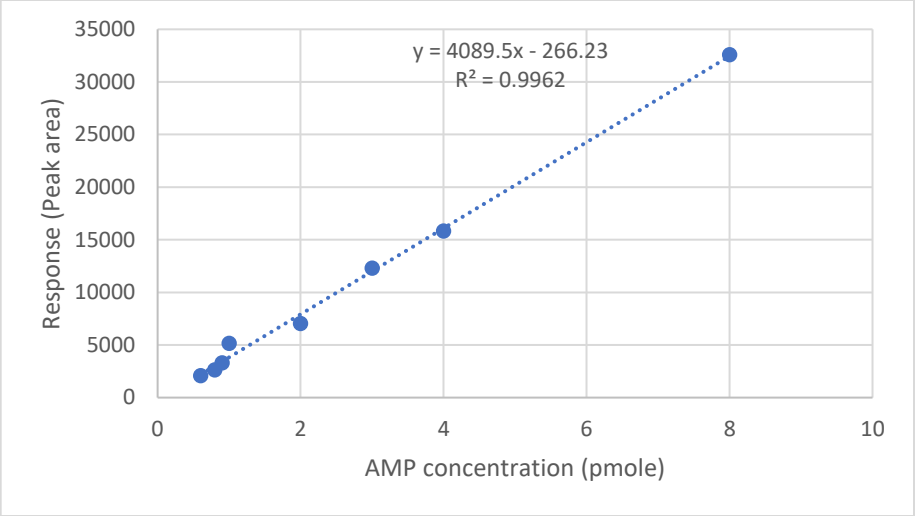

Figure 22: Calibration curve for the quantification of AMP in the range of 0.6 - 8 pmol by LC-MS using the HILIC-ESI-MS method.

2.6.6 ESI-MS/MS fragmentation analysis of NAADP:

In this work, NAADP fragmentation patterns were obtained using tandem high-performance liquid chromatography coupled to a triple quadrupole mass spectrometer with an electrospray ion source (Shimadzu LCMS-8050). When using a triple quadrupole mass spectrometer, specific ions are selected and fragmented by collision-induced dissociation (CID). The collision energy is one main parameter for identification and optimization of the fragmentation pattern, i.e. fragments produced from applying a high voltage in the collision cell. First, 50 pmol of NAADP was directly injected to the LC-MS/MS at a flow rate of 0.2 mL/min. The mobile phase was modified according to the chromatographic elution of NAADP and consisted of 100 % of 10 mM ammonium acetate (pH 9.8). Figure 23 shows the CID spectrum of NAADP from its precursor ion (743 m/z) obtained at a fragmentation voltage of 35 v, heating gas flow of 10 L/min, interface temperature 300 ˚C, and drying gas flow of 10 L/min. The product ions were scanned for from 130 to 660 m/z. Observed fragments were consistent with NAADP fragments obtained by J. Hyun et al. [48] using MS fragmentation strategies including the use of infrared-multiphoton dissociation, electron-induced dissociation, and collision-activated dissociation. Fragment patterns from the NAADP precursor ion shows that the most abundant ions were (408 and 273 m/z), more fragments with lower signal intensities were observed (620, 540, 506 m/z). The proposed fragmentation pattern of NAADP is

shown in Fig. 24. The ion at m/z 620 is attributed to the loss of the nicotinic acid moiety. Dominant observed fragment ions are derived from the phosphate loss. The abundant ion at m/z 408 is a result of the cleavage of the phosphoanhydride bond and loss of the nicotinic acid mononucleotide. The fragment ion at m/z 273 can be attributed to the cleavage of the phosphoanhydride bond along with loss of both the nicotinic acid mononucleotide and the adenine moiety $[408\text{-}A\text{-}H]^-$.

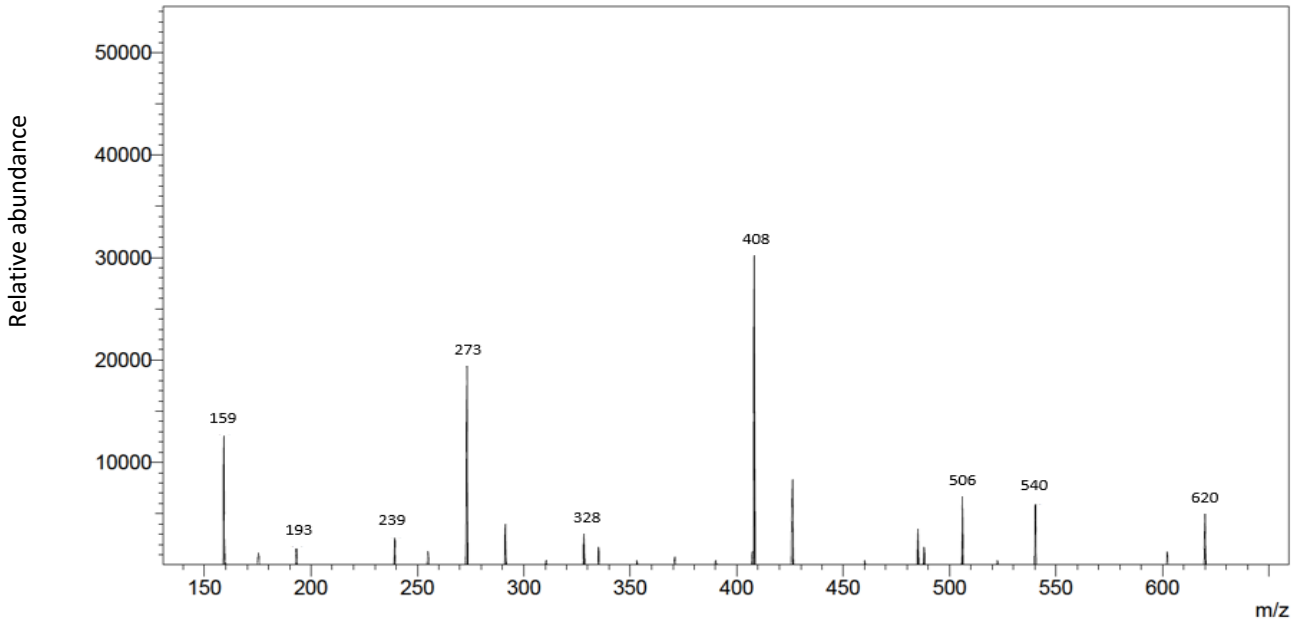

Figure 23: Negative ion MS/MS spectrum showing the NAADP fragment ions from the precursor ion (743 m/z) obtained at a fragmentation voltage of 35 V using LC-MS 8050.

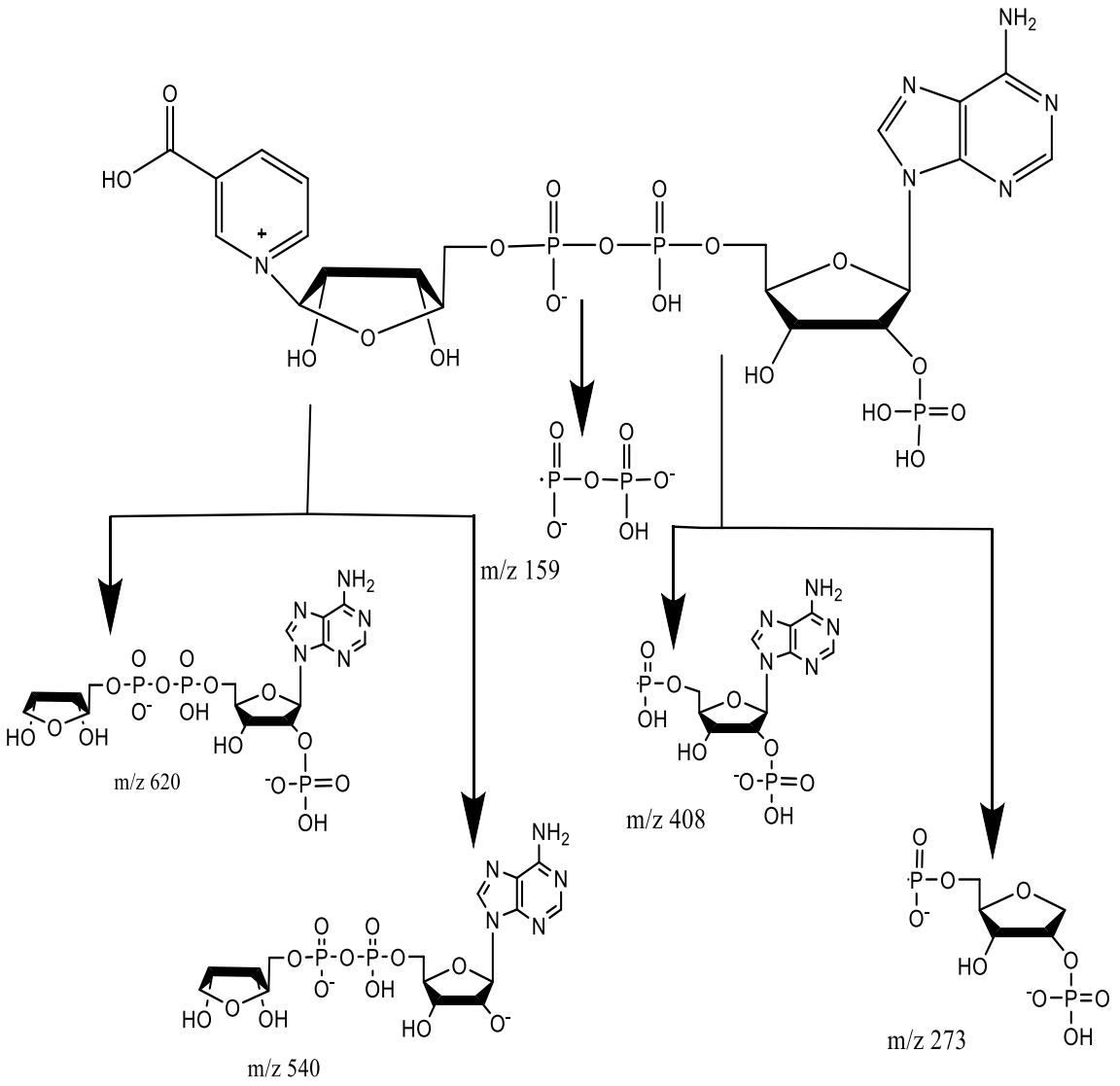

Figure 24: Scheme of the structure and observed MS/MS fragmentation patterns of NAADP (m/z 743) obtained at 35 V. m/z 743 → 620, loss of the nicotinic acid moiety; m/z 743 → m/z 408, cleavage of the phosphoanhydride bond and loss of the nicotinic acid mononucleotide; m/z 743 → m/z 273, cleavage of the phosphoanhydride bond along with the loss of the both nicotinic acid mononucleotide and adenine moiety.

Chapter 3

Conclusion

Obtaining quantitative measurement of NAADP in biological samples is a complicated task. Challenges in separation and detection of endogenous NAADP are mainly related to the high polarity of nucleotides, structural similarities, multiple phosphate moieties of different nucleotides, and the relatively low endogenous NAADP levels as compared to other metabolites. A primary goal was to identify and establish an LC/MS method that enables NAADP analysis in the presence of related nucleotides such as NADP, NAD, ATP, ADP, and AMP. In this work, all stationary chromatographic phases were selected based on the hydrophilic properties of our analyte of interest (NAADP). The utilization of volatile salts and additives was extensively considered for avoiding ion suppression effects during the LC-MS development process. The chromatographic development work was carried out for the both HILIC and RP-HPLC modes. In general, our compounds showed poor retention characteristics on columns in the RPLC methods. In the HILIC mode, the silica HILIC column was able to provide excellent retention properties; however, peaks exhibited very poor shapes.

In contrast, the amino stationary phase in the HILIC mode and at pH 9.8 showed successful retention and separation of NAADP and other nucleotides. The established chromatographic method was optimized and coupled to the LCMS-2020 for both accurate NAADP analysis and detection. The resulting HILIC-MS approach will be a helpful tool for measuring cellular NAADP levels based on the efficient chromatographic separation, molecular ionization, and fragmentation properties that had been established. This work also included the synthesis of D_4-NAADP as an internal standard that would provide traceability and accuracy in the quantitative evaluation of NAADP. This approach has been shown to be a promising new tool for the quantitative measurement of endogenous NAADP.

Cordell et al. were able to develop a method for quantitative profiling of nucleotides using ion-pair reversed-phase LC-MS/MS method [41]; this method offers detection of 5 pmol quantities of NAADP using DMHA as an ion-pairing reagent. In contrast, our method capable of offering a comparable detection sensitivity and has the benefit of avoiding the use of ion-pairing reagents.

On the other hand, available NAADP-measurement assays show sensitive detection

of NAADP, with the ability to detect 50 fmol and 100 amol quantities using the cycling assay and binding assay, respectively. [27,29] The HILIC-MS method that we developed is capable of directly detecting 2 pmol amounts of NAADP.

Basal NAADP levels of 0.14 pmol/mg protein was determined in red blood cells using the binding assay.[28] For our method, 172 µL of packed cells (43 mg of protein) is required to produce the 6 pmol NAADP needed for quantitation of NAADP in RBCs using the HILIC-MS method (assuming that 100 µL of packed cells contains 25 mg of protein [28]).

Chapter 4

Experimental procedures

4.1 Chromatographic methods for analyzing and separating of NAADP:

The analysis and purification of NAADP were performed using two different anion-exchange chromatography resins. AG MP-1 resin in trifluoroacetate form (purchased from Bio-Rad Laboratories) was packed and fitted into A BioLogic Duoflow HPLC system, and DEAE cellulose resin, DE53, (purchased from Whatman International Ltd) was packed into an open column and used for NAADP desalting and further purification purposes. The analysis of nucleotides using anion-exchange resin (AG MP-1 resin) was originally defined in Axelson et al. [51]

4.1.1 HPLC method 1 (Analytical ion exchange column chromatography):

The analytical ion exchange column (7 mm × 35 mm, 1.3 mL) was purchased from Bio-Rad and packed into a glass column that was empty then fitted to the HPLC system (Bio-Rad) using a BioLogic Duo flow fitting kit. The analytical column was then packed with a prepared AG-MP1 trifluoroacetate form resin using a pipette. After packing, the

column was attached to a pump head to allow water to move through the resin to a waste bottle. Pressure compresses the resin and makes it wet and the column can be opened and more resin are added at the top. This process could be repeated several times to ensure that there was no dead volume at the top of the column.

The analytical ion-exchange chromatography was essential in monitoring the progress of the enzymatic base-exchange reaction. The analytical approach was developed at a flow rate of 3 mL/min. The mobile phase was solvent (A) de-ionized water and solvent (B) 100 mM trifluoroacetic acid, TFA. The HPLC system started with an isocratic flow of 100 % A for 2 min, followed by a linear gradient of 45 % B over 17 minutes, then an isocratic flow of 100 % B for 3 minutes followed by an isocratic flow of solvent A for 3 minutes. Column washing was done after each analytical sample using 100 % of solvent B followed by 35 ml of de-ionized H_20 100 % solvent A for equilibration and the column was ready for the next injection.

4.1.2 HPLC method 2 (preparative ion exchange column chromatography):

A glass column (1.5 cm × 11.5 cm) was packed with Bio-Rad AG MP-1 trifluoroacetate form resin (20 gm) using the same packing procedure that was done with the analytical column in method 1. Separation of NAADP was carried out using 2 mL, or 5 mL washed injecting loops. Solvent (A) was H_2O and solvent (B) was 100 mM trifluoroacetic acid, and the flow rate was adjusted at 6 mL/min. The HPLC system started with an isocratic flow of 100 % solvent A for 5 minutes, followed by a 45 %

linear gradient of solvent B over 30 minutes, then an isocratic flow of 100 % B was applied for 6 minutes. After every run, column washing was performed using 100 % of solvent B followed by re-equilibration with 100 % solvent A.

4.1.3 Open column method 3 diethylaminoethyl cellulose (DEAE-cellulose):

An open column anion-exchange method was used for desalting and further purification of NAADP that had been already purified using the AG MP-1 column **(method 2).** A glass Econo-Column chromatography column (2.5 cm × 50 cm), packed with DE-53 cellulose in 100 mM NH_4HCO_3, was used. The column was equipped with an automated fraction collector and attached to a peristaltic pump. Solvent (A) was deionized H_2O, and solvent (B) was ammonium bicarbonate (600 mM). First, 200 ml of 0.6 M NH_4HCO_3 was run through the column for washing then re-equilibrated with deionized water until the pH of the effluent changed from basic to the neutral condition. Then, dry NAADP can be resuspended in deionized water, 1 mg/15 mL, and loaded onto the column.

4.2 Procedure of synthesis of NAADP using the base exchange reaction:

First, 16 mg of nicotinic acid (0.13 mol) was dissolved in 5 mL of distilled H_2O and transferred to 10 mL vial with stirring bar. The vial was incubated for 30 minutes at 37 °C. After that, pH was adjusted to 4 using diluted NaOH (0.1M), and the mixture incubated again for 10 min at 37 °C. This step was repeated several times until pH was

stabilized at 4. After that,10 mg of NADP (0.013 mmol) was added and the mixture incubated for 10 min before the addition of (36 μg, 180 μL*) Aplysia californa* ADPR cyclase and incubated at 37 °C.

Monitoring the progress of the base exchange reaction was performed using **HPLC method 1**. NAADP retention time using method 1 was 9 minutes, 22 mM TFA. After the reaction was done and NADP exchanged to NAADP, the reaction was quenched by adding 10 ml of distilled H_2O and stored at 4 °C. NAADP separation was performed using the preparative column according to **HPLC method 2**. NAADP eluted at 22 minutes, 26% B, and collected manually into a clean flask. After sample collecting, the pH was neutralized using 0.1-1 M NaOH, and the sample was lyophilized overnight.

After lyophilization, dry NAADP was purified and desalted using the open column anion exchange chromatography, **method 3**. The column was washed first with a stirred 200 mL of 0.6 M ammonium bicarbonate until the effluent pH was basic, then washed with 200 mL of distilled H_2O until the pH changed from basic to the neutral condition, assayed with pH-test strips. The lyophilized sample was then dissolved in distilled water, 10 ml of water for each 1 mg of NAADP, and added to the open chromatographic column. The mobile phase system was solvent (A) 400 mL of the distilled H_20, and solvent (B) 400 mL of 0.6 M of ammonium bicarbonate. The reservoir was attached to a low-pressure pump that could pump the mobile phase to the column which was

connected to an automatic fraction collector that collected fractions in standard 13 mm test tubes. NAADP was detected manually by measuring the absorbance of samples in each test tube at 259 nm. Test tubes that had NAADP were combined, frozen and lyophilized three times until pure NAADP was obtained (3.7 mg, 37 %). The concentration of synthetic NAADP was determined by measuring the absorbance of the diluted sample of NAADP and calculated using the NAD extinction coefficient 18000 M^{-1} cm^{-1}. ^{1}H NMR (600 mHz, D_2O) δ 9.16 (s,1H), 9,08 (d, 1H, *J*=6,2 Hz), 8,78 (d, 1H, *J*=8,8 Hz), 8,45 (s, 1H), 8,25 (s, 1H), 8,10 (m, 1H), 6,20 (d, 1H, *J*=5 Hz), 6,05 (d, 1H, *J*=5.6 Hz), 5,10 (m, 1H),4.60 (m ,1H), 4.50 (s, 1H), 4.10-4,23 (m,7H).

4.3 D_4-NAADP synthesis:

First, (19.8 mg, 0.13 mmol) of D_4-nicotinic acid (purchased from Cambridge Isotope Laboratories, Inc) was dissolved in 5 ml of distilled H_2O and transferred to 10 ml vial with stirring bar. The vial was incubated for 30 minutes at 37 °C. After incubation, the pH of the mixture was adjusted to pH 4 using 0.1 M NaOH, and the mixture incubated again for 10 min at 37 °C. This step was repeated several times until the pH was stabilized at 4. After that, (10 mg, 0.013 mmol) of NADP was added and incubated for 10 min before the addition of (24 μg, 200 μL) *Aplysia California* ADPR cyclase and incubated at 37 °C.

Monitoring the progress of the base exchange reaction was performed according to the **HPLC method 1**. The D_4-NAADP retention time using method 1 was 9 minutes (22 mM TFA). After the reaction was complete and NADP exchanged to D_4-NAADP, the reaction was quenched by adding 10 ml of distilled H_2O and stored at 4 °C. D_4-NAADP purification was performed using the preparative column using **HPLC method 2**. D_4-NAADP peak eluted at 22 minutes (26% B) and collected manually at a clean flask. After sample collecting, the pH was neutralized to 7 using (0.1-1 M NaOH) and lyophilized overnight.

After lyophilization, the D_4-NAADP was purified and desalted using an open column anion exchange chromatography, **method 3**. The column was washed first with a stirred 200 ml of 0.6 M ammonium bicarbonate until effluent pH changed to the basic condition, then washed with 200 mL of distilled H_2O until the effluent pH changed from the basic to the neutral condition, measured using pH-test strips. The lyophilized sample was dissolved in distilled water, 10 ml of water for each 1 mg of D_4-NAADP. The sample was added to the open column. The mobile phase system was solvent (A) 600 mL of the distilled H_20 and solvent (B) 600 mL of 0.6 M of ammonium bicarbonate. The reservoir was attached to a low-pressure pump that could pump the mobile phase to the column which was connected to an automatic fraction collector that collected fractions in standard 13 mm test tubes. D_4-NAADP was detected manually by measuring the absorbance of samples at 259 nm. Test tubes that had D_4-NAADP were combined, frozen and lyophilized three times until pure D_4-NAADP was obtained (4.7 mg, 47%). The

concentration of deuterated NAADP was determined after NMR by measuring the absorbance of the diluted sample of NMR solution and calculated using NAD extinction coefficient 18000 M^{-1} cm^{-1}. ^{1}H NMR (600 MHz, D_2O) δ 8,48 (s, 1H), 8,21 (s, 1H), 6,20 (d, 1H, *J*=5.7 Hz), 6,05 (d, 1H, *J*=5.16 Hz), 5,10 (m, 1H), 4.60 (m ,1H), 4.50 (s, 1H), 4.10-4,23 (m, 7H).

4.4 HPLC instrument:

All HPLC development experiments were performed using a SHIMADZU HPLC system (SHIMADZU USA MANUFACTURING, Inc. Canby, OR, U.S.A) coupled to an Ultraviolet/ Visible detector (SPD-20AV). LCsolution software (copyright 2002) was used to collect and display HPLC chromatograms. All chromatographic separations were performed at room temperature, and analytes were monitored at 260 nm and 280 nm.

4.5 HPLC separations using RP-LC technique:

4.5.1 Atlantis dC18 column:

Atlantis dC18 featured a silica bond stationary phase with di-functionally bonded octadecyl ligands that provided superior retention and selectivity of polar compounds in compared with conventional C18 columns. The aqueous mobile phase was solvent (A) 0.1% formic acid and analytes were eluted with either (B) acetonitrile with 0.1% formic

acid or MeOH. The flow rate was 1 mL/min, and the injection volume was 20 µL. The chromatographic separation was performed at the room temperature. Gradient started at 0 %B , then a linear gradient from 0% to 50% of the organic solvent over 25 min, then held constant for 5 min, decreased to 0% B over 0.1 min, and maintained at 0% B for 20 min to re-equilibrate the initial condition, with a total run of 50 min.

4.5.2 Synergi Fusion-RP column:

A silica column with a low density polar embedded C18 ligand and TMS end-capping that provides separation for mixtures of polar and non-polar compounds. The aqueous mobile phase used was solvent (A) 0.1 % of formic acid and eluted with a gradient of the organic phase (B) acetonitrile with 0.1 % formic acid. The flow rate was 0.25 mL/min, and chromatographic runs started with 0 % B, then a linear gradient from 0 % B to 70 % B within 20 min, and held constant for 5 min then back to the initial condition 0 % B over 0.1 min. The gradient maintained at 0 % B for 18 min, and total run was 43 min. The column was ready and re-equilibrated for the next injection.

4.5.3 Kinetex biphenyl column:

Core-Shell silica bound to biphenyl ligand with TMS end-capping column was tested under isocratic and gradient separations (Table 7). Mobile phases system was solvent (A) 0.1% of aqueous formic acid and (B) acetonitrile with 0.1% of formic acid. The isocratic elution started with 0 % B, then an isocratic flow of 100 % A for 10 min, followed by a

linear gradient 0 % to 20 % B constant for 5 min, then a linear gradient from 20 % to 95 % over 10 min, held constant at 95 % B over 10 min, then back to the initial condition 0 % B over 0.1 min. The gradient maintained at 0 % B for 20 min, and total run was 55 min. The gradient elution started with 0 % B, then a linear gradient from 0 % B to 8 % B within 10 min, then linear from 8 % to 95 % B over 15 min, then held constant for 10 min, then back to the initial condition 0 % B over 0.1 min. The gradient maintained at 0 % B for 20 min, and total run was 55 min. In some cases, acetonitrile was replaced with methanol to mark any retention or selectivity improvements in the chromatographic separation. The injection volume was 20 µl, and all chromatographic separations were performed at room temperature conditions.

4.5.4 Synergi Polar-RP column:

An ether-linked phenyl column with polar end-capping was tested as another phenyl column. This ether-linked phase provides more selectivity and greater retention for polar and aromatic compounds on the reversed phase mode, compared to traditional reversed columns. The aqueous mobile phase was solvent (A) H_2O + 0.1% formic acid and solvent (B) acetonitrile with 0.1 % formic acid. The flow rate set at 0.25 mL/min and the injection volume was 20 µL. The column separations were performed at room temperature conditions. A gradient was started at 0% B, then a linear gradient from 0% B to 20% B within 15 min; followed by a linear gradient from 20 % B to 95 % B over 10 minutes which was then held constant for 5 min, decreased to 0 % B within 0.1 min, and

maintained at 0 % B for 15 minutes to reinstate the initial condition. The overall run time was 45 min, and the column was ready for the next run.

4.6 HPLC separations using HILIC-LC technique:

4.6.1 HILIC Kinetex column:

A Phenomenex silica HILIC column (100 mm × 4.6 mm, core-shell 2.6 µm particle size) was tested in the HILIC mode. The flow rate was 0.25 mL/min, and the injection volume was 20 µl. The aqueous phase solvent (A) was 0.1% formic acid, and organic mobile phase solvent (B) was acetonitrile with 0.1% formic acid. Gradient started at 95% B, followed by a gradient from 95 % to 0 % B over 25 min then held constant at 0 % B for 5 min, increased to 95 % B within 0.1 min, and maintained at 95 % B for 20 min to reinstate the initial condition, and total run was 50 min. All runs were performed at room temperature condition.

4.6.2 LUNA NH2 column:

A Phenomenex LUNA NH2 column was employed in HILIC mode. This amino column is stable at wide pH range, pH 1.5 to 11, as well as under 100% aqueous conditions. The aqueous mobile phase used was A) 10 mM ammonium acetate and pH was adjusted to 9.8 using ammonium hydroxide, the organic solvent was B) acetonitrile and the flow rate adjusted at 0.2 mL/min. The chromatographic run started with 80 % B,

then decreased from 80 % B to 0 % B within 20 minutes, and held constant at 0 % B for 10 min, then back to the initial condition over 0.1 min to be re-equilibrated. The re-equilibration time was 18 min, and total run was 48 min.

4.7 Chemicals:

HPLC-grade acetonitrile was purchased from Pharmco-Aaper (Shelbyville, KY 40065) and HPLC-grade methanol was obtained from Fisher (Fair Lawn, NJ 07410) to perform all HPLC experiments. Optima grade of acetonitrile was purchased from Fisher to carry the LC/MS works. The additive formic acid LC/MS grade with 98% purity was obtained from Fisher. Metabolite standards ATP, ADP, AMP, and NAD were purchased from Sigma-Aldrich (St. Louis, USA). NADP was obtained from Research Product International RPI corp. (410 N. Business Center Dr., Mt. Prospect, IL 60056 USA), and NAADP was obtained through the base exchange reaction that was described in the previous section. The deuterium labeled nicotinic acid (D_4-nicotinic acid, >98 atom %D) was purchased from Cambridge Isotope Laboratories, Inc.

4.8 LC Solvents:

4.8.1 Preparation of 0.1% formic acid (V/V) in water:

Using a clean LC solvent bottle, 1 mL of optima LC/MS grade formic acid (99.5+% v/v) was added to deionized water at a final volume of 1 liter, and solvent A was ready to use.

4.8.2 5 and 10 mM of Ammonium acetate (pH 9.8):

0.385 g and 0.77 g of ammonium acetate were purchased from Fisher Scientific (analysis grade, >98%) and used to prepare 5 mM and 10 mM of ammonium acetate mobile phases, respectively. The required amount of buffer was added to 500 ml of de-ionized water and mixed thoroughly until the salt was completely dissolved. The solvent was filtered using 0.2 µm membrane filter (Nylon). Water was added to 950 mL, and pH was adjusted to (9.8) by using ammonium hydroxide. Water was added at a final volume of 1 L, and pH rechecked before use.

4.9 LC-MS 2020 instrument:

The LC used for this instrument was a SHIMADZU system incorporated two LC-20AT pumps, DGU-20A degassing, SPD-20AV UV/VIS detector, SIL-20A autosampler and column thermostat compartment. The mass spectrometer was a SHIMADZU (Shimadzu Corp.) model LCMS-2020 with a dual ionization source (ESI and APCI).

References

(1) Michell, R. Inositol Phopholipids and Cell Surface Receptor Function. *Elsevier* **1975**, *415*, 81–147.

(2) Michell, R., Kirk, C. K., Jones, L. M., Dowens, C. P., Cerba, J. A. The Stimulation of Inositol Lipid Metabolism That Accompanies Calcium Mobilization in Stimulated Cells : Defined Characteristics and Unanswered Questions. *Philos. Trans. R. Soc.* **1981**, *137*, 123–137.

(3) Berridge, M. J. Inositol Trisphosphate and Calcium Signalling Mechanisms. *BBA - Mol. Cell Res.* **2009**, *1793* (6), 933–940.

(4) Lee, H. C. Pyridine Nucleotide Metabolites Stimulate Calcium Release from Sea Urchin Egg Microsomes Desensitized to Inositol Trisphosphate. *J. Biol. Chem.* **1987**, *262* (20), 9561–9568.

(5) Lee, H. C.; Walseth, T. F.; Bratt, G. T.; Hayes, R. N.; Clapper, D. L. Structural Determination of a Cyclic Metabolite of NAD with Intracellular Ca^{+2}-Mobilizing Activity. *J. Biol. Chem.* **1989**, *264* (3), 1608–1615.

(6) Lee, H. C.; Aarhus, R. ADP-Ribosyl Cyclase : An Enzyme That Cyclizes NAD into a Calcium-Mobilizing Metabolite. *Cell Regul.* **1991**, *2* (March), 203–209.

(7) Hon Cheung Lee; Aarhus, R. A Derivative of NADP Mobilizes Calcium Stores Insensitive to Inositol Trisphosphate and Cyclic ADP-Ribose. *Journal of Biological Chemistry*. 1995, pp 2152–2157.

(8) Lee, H. C. Mechanisms of Calcium Signaling by Cyclic ADP-Ribose and NAADP. *Am. Physiol. Soc.* **1997**, *77* (4), 1133–1164.

(9) Clapham, D. E. Calcium Signaling Review. *Cell Press* **1995**, 259–268.

(10) Galione, A.; Churchill, G. C. Interactions between Calcium Release Pathways : Multiple Messengers and Multiple Stores. *Cell Calcium* **2002**, *32*, 343–354.

(11) Kinnear, N. P.; Boittin, F.; Thomas, J. M.; Galione, A.; Evans, A. M. A Trigger Zone for Calcium Signaling by Nicotonic Acid Adenine Dinucleotide Phosphate and Endothelin-1. *J. Biol. Chem.* **2004**, *279* (52), 54319–54326.

(12) Hao, X.; Tang, J.; Rietdorf, K.; Teboul, L.; Chuang, K.; Lin, P.; Xiao, R.; Wang, C.; Zhu, Y.; Lin, Y.; et al. NAADP Mobilizes Calcium from Acidic Organelles through Two- Pore Channels. *Nature* **2009**, *459* (7246), 596–600.

(13) Zong, X.; Schieder, M.; Cuny, H.; Fenske, S.; Gruner, C.; Rötzer, K.; Griesbeck, O.; Harz, H.; Biel, M.; Wahl-schott, C. The Two-Pore Channel TPCN2 Mediates NAADP-Dependent Ca^{+2}-Release from Lysosomal Stores. *Eur. J. Physiol.* **2009**, *458*, 891–899.

(14) Cancela, J. M.; Churchill, G. C.; Galione, A. Letters to Nature Coordination of Agonist- Induced Ca^{+2}-Signalling Patterns by NAADP in Pancreatic Acinar Cells. *Curr. Biol.* **1999**, *9* (14), 751–754.

(15) Bak, J.; White, P.; Timár, G.; Missiaen, L.; Genazzani, A. A.; Galione, A. Nicotinic Acid Adenine Dinucleotide Phosphate Triggers Ca^{+2} Release from Brain Microsomes. *Curr. Biol.* **1999**, *9*, 751–754.

(16) Lee, H. C.; Aarhus, R. Functional Visualization of the Separate but Interacting Calcium Stores Sensitive to NAADP and Cyclic ADP-Ribose. *Cell Sci.* **2000**, *4420*, 4413–4420.

(17) Churchill, G. C.; Okada, Y.; Thomas, J. M.; Genazzani, A. A.; Patel, S.; Galione, A. NAADP Mobilizes Ca^{+2} from Reserve Granules , Lysosome-Related Organelles , in Sea Urchin Eggs. *Cell Press* **2002**, *111*, 703–708.

(18) Petersen, O. H. Ca^{+2} Signalling and Ca^{+2}-Activated Ion Channels in Exocrine Acinar Cells. *Cell Calcium* **2005**, *38*, 171–200.

(19) Brailoiu, E.; Churamani, D.; Cai, X.; Schrlau, M. G.; Brailoiu, G. C.; Gao, X.; Hooper, R.; Boulware, M. J.; Dun, N. J.; Marchant, J. S.; et al. Essential Requirement for Two-Pore Channel 1 in NAADP-Mediated Calcium Signaling. *Cell Biol.* **2009**, *186* (2), 201–209.

(20) Zhu, M. X.; Ma, J.; Parrington, J.; Calcraft, P. J.; Galione, A.; Evans, A. M. Calcium Signaling via Two-Pore Channels : Local or Global , That Is the Question. *Am. J. Physiol.* **2019**, No. 39, 430–441.

(21) Bak, J.; Billington, R. A.; Timar, G.; Dutton, A. C.; Genazzani, A. A. NAADP Receptors Are Present and Functional in the Heart. *Curr. Biol.* **2001**, *11*, 987–990.

(22) Lewis, A. M.; Aley, P. K.; Roomi, A.; Thomas, J. M.; Masgrau, R.; Garnham, C.; Shipman, K.; Paramore, C.; Bloor-young, D.; Sanders, L. E. L.; et al. Biochemical and Biophysical Research Communications SS-Adrenergic Receptor Signaling Increases NAADP and CADPR Levels in the Heart. *Elsevier* **2012**, *427*, 326–329.

(23) Berg, I.; Potter, B. V. L.; Mayr, G. W.; Guse, A. H. Nicotinic Acid Adenine Dinucleotide Phosphate (NAADP) Is an Essential Regulator of T-Lymphocyte Ca^{+2}-Signaling. *J. Cell Biol.* **2000**, *150* (3), 581–588.

(24) Ali, R. A.; Camick, C.; Wiles, K.; Walseth, T. F.; Slama, J. T.; Bhattacharya, S.; Giovannucci, D. R.; Wall, K. A. Nicotinic Acid Adenine Dinucleotide Phosphate Plays a Critical Role in Naive and Effector Murine t Cells but Not Natural Regulatory t Cells. *J. Biol. Chem.* **2016**, *291* (9), 4503–4522.

(25) Davis, L. C.; Morgan, A. J.; Chen, J.; Snead, C. M.; Bloor-young, D.; Shenderov, E.; Stanton-humphreys, M. N.; Conway, S. J.; Churchill, G. C.; Parrington, J.; et al. Report NAADP Activates Two-Pore Channels on T Cell Cytolytic Granules to Stimulate Exocytosis and Killing. *Curr. Biol.* **2012**, *22* (24), 2331–2337.

(26) Graeff, R.; Lee, H. C. An Improved Enzymatic Cycling Assay for NAADP. *Am. Sci. Publ.* **2013**, *2*, 96–105.

(27) Gasser, A.; Bruhn, S.; Andreas, H.; Gasser, A. Second Messenger Function of

Nicotinic Acid Adenine Dinucleotide Phosphate Revealed by an Improved Enzymatic Cycling Assay. *J. Biol. Chem.* **2006**, *281*, 16906–16913.

(28) Churamani, D.; Carrey, E. A.; Dickinson, G. D.; Patel, S. Determination of Cellular Nicotinic Acid–Adenine Dinucleotide Phosphate (NAADP) Levels. *Biochem. J.* **2004**, *454*, 449–454.

(29) Lewis, A. M.; Masgrau, R.; Vasudevan, S. R.; Yamasaki, M.; Neill, J. S. O.; Garnham, C.; James, K.; Macdonald, A.; Ziegler, M.; Galione, A.; et al. Refinement of a Radioreceptor Binding Assay for Nicotinic Acid Adenine Dinucleotide Phosphate. *Anal. Biochem.* **2007**, *371*, 26–36.

(30) Graeff, R.; Lee, H. C. A Novel Cycling Assay for Cellular CADP-Ribose with Nanomolar Sensitivity. *J. Biochem.* **2002**, *384*, 379–384.

(31) Pitt, J. J. Principles and Applications of Liquid Chromatography-Mass Spectrometry in Clinical Biochemistry. *Clin. Biochem. Rev.* **2009**, *30* (1), 19–34.

(32) Hardie, D. G.; Hawley, S. A. AMP-Activated Protein Kinase: The Energy Charge Hypothesis Revisited. *BioEssays* **2001**, *23* (12), 1112–1119.

(33) Vanlinden, M. R.; Skoge, R. H.; Ziegler, M. Discovery , Metabolism and Functions of NAD and NADP. *Biochem. (Lond).* **2015**, *37* (1), 9–13.

(34) Manuscript, A.; Magnitude, S. Regulation of Cell Survival and Death by Pyridine Nucleotides. *NIH Public Access* **2013**, *31* (9), 1713–1723.

(35) Robert Pellecchia, Curtis Holmes, G. B. and F. R. S. Mass Spectrometry for the Sensitive Analysis of Intracellular Nucleotides and Analogues. *A Textb. Adv. Oral Maxillofac. Surg.* **2017**, *3*, 135–185.

(36) Cohen, S.; Jordheim, L. P.; Megherbi, M.; Dumontet, C.; Guitton, J. Liquid Chromatographic Methods for the Determination of Endogenous Nucleotides and Nucleotide Analogs Used in Cancer Therapy: A Review. *J. Chromatogr. B Anal. Technol. Biomed. Life Sci.* **2010**, *878* (22), 1912–1928.

(37) Nakanishi, T.; Hishiki, T.; Morikawa, T.; Kajimura, M.; Suematsu, M. Simultaneous Analysis of Primary Metabolites by Triple Quadrupole LC/MS/MS . Primary Metabolites LC/MS/MS Method Package. *Shimadzu Rev.* **2013**, *SR14_007E*.

(38) Klawitter, J.; Schmitz, V.; Klawitter, J.; Leibfritz, D.; Christians, U. Development and Validation of an Assay for the Quantification of 11 Nucleotides Using LC/LC-Electrospray Ionization-MS. *Anal. Biochem.* **2007**, *365* (2), 230–239.

(39) Michopoulos, F.; Whalley, N.; Theodoridis, G.; Wilson, I. D.; Dunkley, T. P. J.; Critchlow, S. E. Targeted Profiling of Polar Intracellular Metabolites Using Ion-Pair-High Performance Liquid Chromatography and -Ultra High Performance Liquid Chromatography Coupled to Tandem Mass Spectrometry: Applications to Serum, Urine and Tissue Extracts. *J. Chromatogr. A* **2014**, *1349*, 60–68.

(40) Luo, B.; Groenke, K.; Takors, R.; Wandrey, C.; Oldiges, M. Simultaneous Determination of Multiple Intracellular Metabolites in Glycolysis, Pentose Phosphate Pathway and Tricarboxylic Acid Cycle by Liquid Chromatography-Mass Spectrometry. *J. Chromatogr. A* **2007**, *1147* (2), 153–164.

(41) Cordell, R. L.; Hill, S. J.; Ortori, C. A.; Barrett, D. A. Quantitative Profiling of Nucleotides and Related Phosphate-Containing Metabolites in Cultured Mammalian Cells by Liquid Chromatography Tandem Electrospray Mass Spectrometry. *J. Chromatogr. B Anal. Technol. Biomed. Life Sci.* **2008**, *871* (1), 115–124.

(42) Annesley, T. M. Ion Suppression in Mass Spectrometry. *Clin. Chem.* **2003**, *49* (7), 1041–1044.

(43) Bajad, S. U.; Lu, W.; Kimball, E. H.; Yuan, J.; Peterson, C.; Rabinowitz, J. D. Separation and Quantitation of Water Soluble Cellular Metabolites by Hydrophilic Interaction Chromatography-Tandem Mass Spectrometry. *J. Chromatogr. A* **2006**, *1125* (1), 76–88.

(44) Seifar, R. M.; Ras, C.; Deshmukh, A. T.; Bekers, K. M.; Suarez-Mendez, C. A.; da Cruz, A. L. B.; van Gulik, W. M.; Heijnen, J. J. Quantitative Analysis of Intracellular Coenzymes in Saccharomyces Cerevisiae Using Ion Pair Reversed Phase Ultra High Performance Liquid Chromatography Tandem Mass Spectrometry. *J. Chromatogr. A* **2013**, *1311*, 115–120.

(45) Alpert, A. J. Hydrophilic-Interaction Chromatography for the Separation of Peptides, Nucleic Acids and Other Polar Compounds. *J. Chromatogr. A* **1990**, *499* (C), 177–196.

(46) Bustamante, S.; Jayasena, T.; Richani, D.; Gilchrist, R. B.; Wu, L. E.; Sinclair, D. A.; Sachdev, P. S.; Braidy, N. Quantifying the Cellular NAD Metabolome Using a Tandem Liquid Chromatography Mass Spectrometry Approach. *Metabolomics* **2018**, *14* (1), 1–15.

(47) Creek, D. J.; Jankevics, A.; Breitling, R.; Watson, D. G.; Barrett, M. P.; Burgess, K. E. V. Toward Global Metabolomics Analysis with Hydrophilic Interaction Liquid Chromatography-Mass Spectrometry: Improved Metabolite Identification by Retention Time Prediction. *Anal. Chem.* **2011**, *83* (22), 8703–8710.

(48) Hyun, J. Y.; Liu, H.; Håkansson, K. Infrared Multiphoton Dissociation and Electron-Induced Dissociation as Alternative MS/MS Strategies for Metabolite Identification. *Anal. Chem.* **2007**, *79* (20), 7858–7866.

(49) Aarhus, R.; Graeff, R. M.; Dickey, D. M.; Walseth, T. F.; Lee, H. C. ADP-Ribosyl Cyclase and CD38 Catalyze the Synthesis of a Calcium-Mobilizing Metabolite from NADP. *J. Biol. Chem.* **1995**, *270* (51), 30327–30333.

(50) Konermann, L.; Ahadi, E.; Rodriguez, A. D.; Vahidi, S. Unraveling the Mechanism of Electrospray Ionization. *Anal. Chem.* **2013**, *85* (1), 2–9.

(51) Axelson, T. B. J. W. T. A Volatile Liquid Chromatography System for Nucleotides. *Anal. Biochem.* **1981**, *116*, 357–360.

Appendix A

NMR results

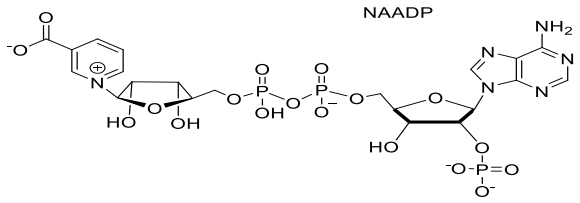

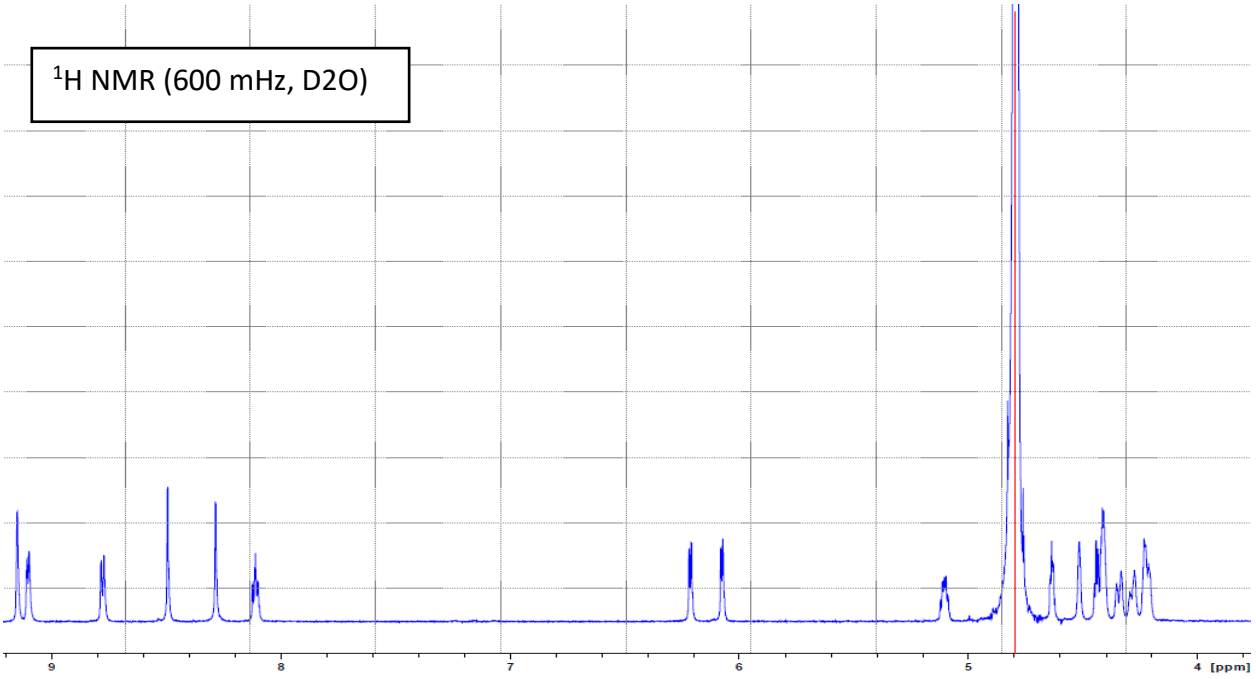

1H NMR spectrum of NAADP (600 MHz, D2O)

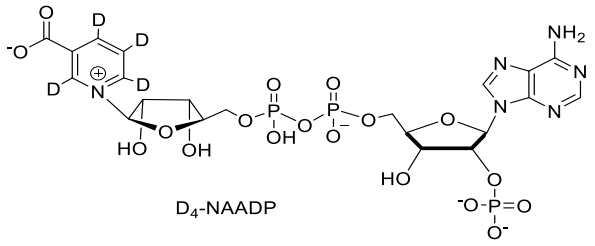

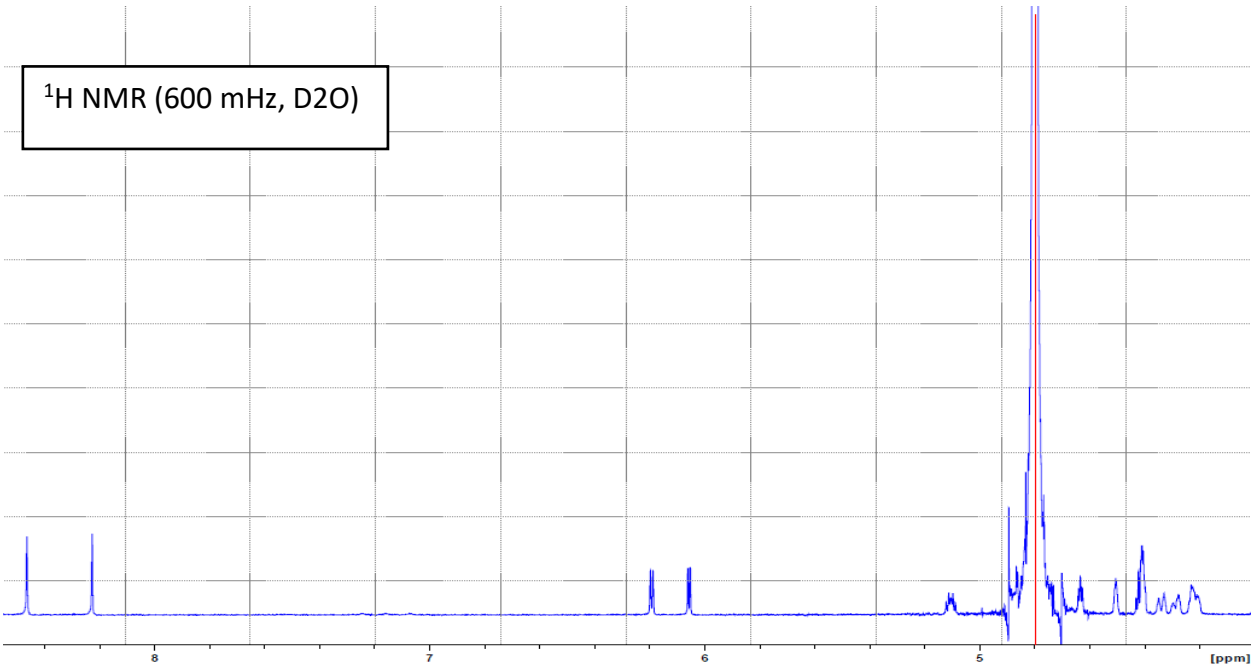

^{1}H NMR spectrum of D_4-NAADP (600 MHz, D2O)